



NACA RM E56B23

5569

# NACA

## RESEARCH MEMORANDUM

HEAT REQUIREMENTS FOR ICE PROTECTION OF A CYCLICALLY  
GAS-HEATED, 36° SWEEP AIRFOIL WITH PARTIAL-SPAN  
LEADING-EDGE SLAT

By Vernon H. Gray and Uwe H. von Glahn

Lewis Flight Propulsion Laboratory  
Cleveland, Ohio

Classification cancelled (or changed to *UNCLASSIFIED*)

By Authority of *NASA Tech Rep. Administration FIR*  
(OFFICER AUTHORIZED TO CHANGE)

By *16 Aug 57*  
NAME AND

*HHB*  
GRADE OF OFFICER MAKING CHANGE

*31 May 61*  
DATE

NATIONAL ADVISORY COMMITTEE  
FOR AERONAUTICS

WASHINGTON

May 14, 1956



## NATIONAL ADVISORY COMMITTEE FOR AERONAUTICS

RESEARCH MEMORANDUMHEAT REQUIREMENTS FOR ICE PROTECTION OF A CYCLICALLY GAS-HEATED,  
36° SWEEP AIRFOIL WITH PARTIAL-SPAN LEADING-EDGE SLAT

By Vernon H. Gray and Uwe H. von Glahn

## SUMMARY

Heating requirements for satisfactory cyclic de-icing over a wide range of icing and operating conditions have been determined for a gas-heated, 36° swept airfoil of 6.9-foot chord with a partial-span leading-edge slat. Comparisons of heating requirements and effectiveness were made between the slatted and unslatted portions of the airfoil. Studies were also made comparing cyclic de-icing with continuous anti-icing, and cyclic de-icing systems with and without leading-edge ice-free parting strips. De-icing heat requirements were approximately the same with either heated or unheated parting strips because of the aerodynamic effects of the 36° sweep angle and the spanwise saw-tooth profile of leading-edge glaze-ice deposits. Cyclic de-icing heat-source requirements were found to be one-fourth or less of the heat requirements for complete anti-icing. The primary factors that affected the performance of the cyclic de-icing heating system were ambient air temperature, heat distribution, and thermal lag.

## INTRODUCTION

The NACA Lewis laboratory has studied several hot-gas icing protection systems in order to obtain data useful in the design of such systems (refs. 1 to 4). In some of these studies, the technique of cyclic de-icing was investigated to determine the heat-flow savings that result from intermittent heating of a portion of an airfoil surface subject to icing as compared with continuous heating of the surface. In evaluating the heat-flow savings resulting from cyclic de-icing, the airfoil drag caused by the ice formations that accrue on the surfaces between heating periods must be considered. The drag penalties for several airfoil shapes and ice-protection techniques have already been obtained (refs. 3, 5, 6, and 7), including the drag study (ref. 5) of the airfoil model used in the present investigation.

In the present study, the heat requirements and effectiveness of a hot-gas cyclic de-icing system in a 36°-swept-airfoil model with a

3081

CS-1

leading-edge slat have been investigated. The model utilized an NACA 63A-009 airfoil section with a slatted leading edge over only a portion of the span. This feature was incorporated to compare simultaneously the heating and icing characteristics of the slatted section with those of the unslatted airfoil. The model was provided also with both hot gas and electrically heated strips along the leading edges in order to determine the effect of continuously heated ice-free parting strips on de-icing performance.

The airfoil model was studied over a range of icing conditions in the NACA Lewis laboratory icing tunnel. Ice-removal data were obtained for the swept-back model, and a study was made of the special problems associated with de-icing of a movable leading-edge slat. The model, furnished by an aircraft manufacturer, was the first hot-gas cyclic de-icing system to be developed for production. In an effort to correct some heating deficiencies that became evident during the tests, modifications of the original internal heating arrangements were made, and limited data on the over-all effects of these changes were obtained.

#### MODEL AND EQUIPMENT

The model used in this study (fig. 1) is a constant-section NACA 63A-009 airfoil which spans the 6-foot height of the icing research tunnel. The leading and trailing edges of the model are swept back at an angle of  $36^{\circ}$  to the airstream. The airfoil structure and heating passages were constructed either perpendicular or parallel to the leading edge. However, in this report, chordwise dimensions will be taken parallel to the airstream and spanwise dimensions parallel to the leading edge. The streamwise airfoil chord was 6.9 feet.

The airfoil leading-edge section consists of two main parts: an unslatted or "standard-airfoil" section with a spanwise extent of approximately 26 inches and a slatted leading-edge section with a spanwise extent of 44 inches. The relation of the movable slat to the fixed-airfoil section behind the slat is shown in figure 2. Slat extension is normally associated with large angles of attack.

#### Slat

The leading-edge slat has a 20-inch chord in the streamwise direction (fig. 1(a)). The slat moves forward on tracks and rollers into the airstream in a direction normal to the leading edge. For the tests, a hydraulic system moves and holds the slat in any desired forward position. The slat tracks are curved so that the extended slat moves on a circular arc to positions forward of and below the lower surface of the fixed-airfoil section (fig. 2(a)). The radius of curvature of the tracks is approximately 34 inches, and the full movement of the slat is over a  $16^{\circ}$  central angle.

3081

Original version. - In the original model version, for which the majority of the data were obtained, the upper and lower surfaces of the slat were gas-heated (figs. 2 and 3). Hot gas was introduced by means of a jointed, swiveling tube into a D-duct which runs spanwise near the leading edge of the slat (figs. 1(b), 2(b), 3(a), and 3(b)). To prevent overheating of the leading-edge surface at the entrance point of the supply duct, a short baffle was positioned to deflect the gas flow spanwise in both directions (figs. 3(a) and (b)). The hot gas was then distributed to both ends of the slat, passed through spanwise double skins in the upper slat surface, and exhausted into the center of the slat through small orifices. In addition, a series of six holes in the D-duct supplied hot gas to the inside of the slat. A portion of the rear face of the slat (slat surface contacting fixed airfoil when slat is retracted) was provided with a double skin to increase the heat transfer (fig. 3(b)). The trailing lip of the lower surface was heated by an extension of this double skin as well as by conduction from the D-duct. The three tabs (fig. 1(b)) were heated by conduction only.

3082

The slat leading edge was provided with an electrically heated ice-free parting strip. The heating unit consisted of an element secured to a spanwise fin which in turn was riveted to the airfoil skin at the stagnation region for normal cruise angle of attack (fig. 3(b)). Electric heating units were also secured around the periphery of the closing ribs at the spanwise ends of the slat (figs. 2(b) and 3(c)) and along the slat tracks (fig. 3(c)).

Modified version. - An insulating fiberglass liner was inserted into the D-duct in the modified version of the slat (fig. 3(e)). The electric heating elements were removed, except for those along the tracks. These latter heaters were altered as shown in figure 3(d) with heating applied only to the side exposed to impingement. The closing ribs were reversed from the original positions so the flanges would not protrude toward the air gaps at the slat ends (fig. 3(c) and (d)). The gas-flow circuit through the slat upper surface was changed to that shown in figure 3(e). In addition to the spanwise-flow pattern of the original version (fig. 3(a)), chordwise gas flow was induced across the first two spanwise passages aft of the D-duct. This flow was accomplished by means of milled spacers along the rivet lines, which provided a small opening between the outer skin and the corrugations of the gas passages; thereby, some gas was allowed to flow chordwise from the D-duct into the next two passages. The lower-surface trailing lip and tabs were heated directly from the D-duct by gas flow through a milled spacer bar. The double skin was removed from the slat rear face.

#### Fixed Airfoil Behind Slat

Partitions perpendicular to the leading edge divided the fixed-airfoil section behind the slat into four heating zones (see fig. 1(b))

7

necessitated by the location of the two slat tracks and the hot-gas duct to the slat. Each zone was gas-heated by means of a small supply duct from a common header, a spanwise D-duct, and double-skin flow passages.

Original version. - A section through one of the heating zones normal to the leading edge is shown in figure 4(a). Double-skin passages were provided on both the top and bottom surfaces. Electric heating elements were used in each zone to obtain an ice-free parting strip near the normal cruise stagnation region of this airfoil section when the slat was extended. Between the four heating zones, lower-surface double-skin constructions extended spanwise over the areas of the tracks and the slat gas-supply duct and were heated by gas fanning out from both adjacent gas-flow passages.

Modified version. - For the modified fixed-airfoil section, the electric parting-strip elements were removed. The upper-surface double skin was eliminated whereas the lower-surface double skin was extended nearer the leading edge (fig. 4(b)). The reinforcement at the airfoil nose that isolated the leading-edge region from gas flow in the original version was removed. In the modified version, greater gas flow was induced in the lower-surface double skins over the slat-track and gas-supply-duct areas by increasing the size of the outlet orifices in the gas-flow passages.

#### Standard-Airfoil Section

Original version. - The standard-airfoil section, which constituted the part of the model near the tunnel floor (figs. 1 and 2), is shown in cross section in figure 5(a). This section was heated by means of gas passages in the double skin, which extended from the leading edge to approximately 22-percent chord on the lower surface and 15-percent chord on the upper surface. Gas flow to these double skins was supplied through a leading-edge spanwise D-duct. There are no ribs located forward of the front span as the stresses are carried by a structural inner skin corrugated to conform with the corrugations of the flow passages.

In the original standard airfoil, a gas-heated parting strip was provided in the form of a small circular duct (1/2-in. I.D.) secured to a fin which was riveted to the outer skin at the cruise stagnation region (fig. 5(a)). The parting-strip gas supply was independent of the gas supply to the double-skin passages. The D-duct areas were partly lined with fiberglass insulation to conserve heat. The passage height between double skins was tapered from 5/16 inch at the inlet to 3/32 inch at the outlet. This tapering promotes more uniform surface heating by increasing the internal heat-transfer coefficient to offset the diminishing temperature of the gas. The closing rib adjacent to the slat was electrically heated in a manner similar to that of the slat shown in figure 3(c) to prevent ice bridging across to the slat.

Modified version. - In the modified standard-airfoil section (fig. 5(b)) the gas-heated parting strip was removed and the D-duct supplied with a tubular fiberglass insert to replace the sheet insulation of the original model. The remainder of the standard airfoil was the same as the original model.

#### Other Items of Equipment

3081 For the original model only, the following surface areas abutting the fixed-airfoil section were heated to prevent ice deposits (see fig. 1(b)): (a) the triangular area between the fixed-airfoil upper extremity and the top of the model was provided with a double skin and supplied with an independent, manually operated source of hot gas; and (b) the triangular area between the standard- and the fixed-airfoil sections was provided with a constant-gap double skin and supplied with hot gas from the standard-airfoil supply duct. Between the standard-airfoil section and the tunnel floor was a small triangular area (fig. 1(a)) which remained unheated during the tests.

The three airfoil sections of the model were capable of being heated independently for cyclic ice removal or collectively for continuous anti-icing.

Cycling of the hot gas was accomplished by the use of double-throated valves with two butterfly plates displaced  $90^\circ$  on a common shaft. The valves were pneumatically operated and controlled by solenoids. In order to maintain steady gas flow, the cycling valves would divert the flow into the tunnel downstream of the model when not delivering gas to the leading-edge sections.

Surface and gas temperatures were obtained by thermocouples dispersed throughout the original model and connected to recording potentiometers. The modified model was equipped with a limited number of thermocouples. The main planes of surface-temperature instrumentation are shown in figure 1(b). The painted lines shown on the model in figure 1 were used as guides in recording the location and extent of icing during the tests.

Electrical heating rates were obtained from wattmeters. Gas-flow rates into each airfoil section were obtained by means of calibrated orifices and venturi tubes in the supply ducts. Flow metering both upstream and downstream of the cycling valves detected any leakage at the valve. Hot-gas supply temperatures were obtained by thermocouples mounted in the duct just upstream of the cycling valves. The approximate duct lengths between the cycling valves and the D-duct entrances were as follows: slat,  $5\frac{1}{2}$  feet; fixed airfoil,  $7\frac{1}{2}$  feet; standard airfoil, 6 feet.

## CONDITIONS AND PROCEDURE

## Range of Conditions

The range of conditions in this study was

Airspeed, mph . . . . .	175 and 260
Liquid-water content, gm/cu m . . . . .	0.3 to 1.3
Total air temperature, °F . . . . .	0 to 29
Cycling-valve inlet gas temperature, °F . . . . .	300 and 450

The geometric angle of attack of the airfoil was varied from 0° to 8° with the slat fully retracted; with the slat extended 8° (half of maximum travel), the angle of attack for the airfoil was set at 8°. A study was also made at an angle of attack of 12° with the slat half extended (8°) and fully extended (16°). The studies with slat extended were made at an airspeed of 175 mph.

## Procedure for Obtaining Data

In obtaining data during a de-icing run, the procedure was to establish first the tunnel conditions of airspeed and air temperature and then the heating conditions of both gas flow and gas temperature (at the cycling valves). The gas flows were stabilized while the cycling valves were positioned to dump the gas flow into the tunnel. Then, water sprays were turned on and the cycle timers were started simultaneously to control selected icing and heating periods. Generally, the first cycle started with the icing period and followed with the heating (de-icing) period.

In order to determine heating requirements, the first few icing cycles were utilized to adjust the heating rates until satisfactory de-icing was obtained. For convenience, the heat-on times were adjusted (with other conditions constant) until satisfactory ice shedding performance was obtained.

Satisfactory de-icing performance was determined by visual observation and then the model was photographed at significant moments in the cycle. The criterion of satisfactory, or marginal, de-icing was selected as the condition of complete ice removal from an airfoil section as far aft as the limit of the heatable double skin. This criterion was compromised in certain local areas that were inadequately heated, and consequently, some ice formations which were local in nature would not shed and were ignored as much as possible in establishing marginal levels of heating. This criterion, unavoidably subjective in nature, caused considerable scatter in the data.

Operation of the parting strips was considered satisfactory when the leading-edge strips would remain ice-free over an average chordwise distance of approximately 1/2 inch after a 4- to 6-minute icing period.

Anti-icing heat requirements were determined for the condition of an ice-free model for which the impinging water either evaporated on the heated areas or ran off the surface before freezing. Water run-off was frequently observed at the trailing lip of the slat lower surface.

#### Method of Presenting Data

In order to establish a convenient reference temperature from which to compute heat transfer in the tunnel, a datum air temperature was taken as the average unheated surface temperature of the airfoil leading-edge sections. In icing conditions, the datum temperature was taken from readings that were not affected by the heat of fusion of impinged water (fig. 5, ref. 2). The datum air temperature was essentially equal to the total air temperature within  $1\frac{1}{2}^{\circ}$  F for the conditions investigated.

During the heat-on period, the gross heating rates per foot of span are given by

$$q = Wc_p(t_g - t_d), \text{ Btu}/(\text{hr})(\text{ft span}) \quad (1)$$

where

$q$  gross heating rate per foot span

$W$  gas flow, lb/(hr)(ft span)

$c_p$  specific heat of air at constant pressure, 0.24 Btu/(lb)( $^{\circ}$ F)

$t_g$  gas temperature at cycling valve,  $^{\circ}$ F

$t_d$  datum air temperature,  $^{\circ}$ F

These heating rates are based on spanwise lengths along the leading edges and exclude the various triangular areas mentioned previously. The heating values include the heat losses in the supply ducts between the cycling valves and the D-duct entrances.

In order to compare intermittent heating rates with anti-icing heating rates, the heating rate for cyclic de-icing is divided by the cycle ratio to obtain an "equivalent-continuous heating rate." The ratio of

total cycle time to the heat-on time is defined as the "cycle ratio." The heating rates per foot span for ice-free parting strips are included in the equivalent-continuous heating rates for the entire specified airfoil section. The heating rates for gas-heated parting strips are presented as the product of total gas flow, specific heat, and the gas temperature drop per foot span. For the electric parting strips, the heating rates are determined from the total required wattage divided by total effective span.

In the presentation of surface temperatures, unless otherwise stated, the temperatures are measured along rivet lines where the outer and inner skins join.

## RESULTS AND DISCUSSION

The results are presented in two parts. The first part is concerned with the over-all performance of the de-icing systems, and the second presents several aspects of local and internal heat-transfer processes.

### Over-All Performance of De-Icing Systems

Characteristic glaze-ice deposits. - Glaze icing on the unheated model is shown in figures 6(a) and (b) with slat retracted and fully extended, respectively, and in figure 6(c) with the slat half extended and only the parting strips heated. It was observed during the tests that the ice-free parting strips did not appreciably alter the shape of the rest of the ice formation at the nose.

The photographs in figure 6 illustrate a peculiarity of leading-edge glaze ice on swept airfoils. Whereas ice on unswept airfoils forms continuous spanwise projections of uniform shape along the leading edge (ref. 2), the ice forms in a discontinuous, saw-tooth fashion on swept airfoils such as the present one. In rime-icing conditions, there is no difference in appearance of the ice on swept and unswept airfoils (ref. 5).

Areas of insufficient heating. - With cyclic application of heat to the model, residual ice formations indicate local regions of insufficient heating. With the slat extended, the tracks were insufficiently heated even at a datum air temperature of 25° F and an airspeed of 175 mph. The rear face of the slat (figs. 1(b) and 2(a)) was virtually unprotected by the cyclic de-icing system and accumulated sizable ice formations (fig. 7(a)). These ice formations decreased the exit area of the slot between the slat and fixed airfoil and often prevented complete slat retraction by as much as 3 inches of travel. Similarly, runback icing formed on the last 4 inches of the slat trailing edge on the upper surface and

could not be dislodged except by excessive amounts of heat. The large ice masses on the slat tabs (fig. 7(a)) could only be removed by exorbitant heating. With marginal heating, these ice formations would grow for four to six heating cycles and then shed sporadically. The closing ribs at the slat ends were insufficiently protected at datum air temperatures less than 20° F.

The fixed-airfoil section behind the slat was inadequately protected at the leading-edge region by the electric parting strips. A nonuniform distribution of gas heating to the lower surface of this fixed section caused several cold areas. These areas accumulated massive ice formations, especially near the track openings and on the airfoil skin over the track stations (fig. 7(a)). At low datum air temperatures with slat extended, ice formed on the insulated gas supply duct to the slat.

The standard-airfoil portion of the model showed a rapid reduction in the width of the gas-heated parting strip in the direction of gas flow. In addition, a surface strip between the skin junction with the parting-strip fin and the entrance to the upper-surface double skin was inadequately heated. This caused an ice ridge to remain near the leading edge after the rest of the airfoil was cleanly de-iced.

The unheated or poorly heated regions of the modified model can be seen in figure 7(b). Although figures 7(a) and (b) illustrate residual icing under different icing conditions, generally the same areas are under-heated in the modified version as in the original model. This illustrates the difficulty of heating certain localized areas because of structural complications. The modified model, however, showed marked improvement over the original version in the de-icing of the slat tracks, the slat trailing lip, and the leading-edge regions of the fixed- and standard-airfoil sections. The improved ice protection for the tracks, however, was largely offset by the ice that built up (on both versions of the model) on the unheated areas near the track openings in the fixed airfoil.

Marginal de-icing. - Typical operation of the various de-icing systems in the models is shown in figures 8 and 7(b). Figures 8(a) and (b) show de-icing of the airfoils in glaze-icing conditions (airspeed, 260 mph) for the original and modified models, respectively, whereas figures 8(c) and 7(b) (airspeed, 175 mph) can be compared for operation in rime-icing conditions. The heat-on periods and heating rates for these examples of marginal de-icing are given in the following tabulation for the three airfoil sections of the model:

Fig- ure	Icing condi- tion	Heat- off peri- od, min	Heat-on period, sec			Heating rate, Btu/(hr) (ft span)			Parting-strip heating rate, Btu/(hr) (ft span)		
			Stand- ard	Slat	Fixed	Stand- ard	Slat	Fixed	Stand- ard	Slat	Fixed
8(a)	Glaze	$3\frac{1}{2}$	19	15	15	18,200	18,125	14,600	226	140	252
8(b)	Glaze	$3\frac{5}{6}$	10	10	10	20,375	21,597	15,168	---	---	---
8(c)	Rime	3	27	27	30	18,100	15,900	17,350	378	280	630
7(b)	Rime	$3\frac{1}{4}$	15	15	15	24,204	20,584	16,197	---	---	---

The ice formations remaining on the model after the heating periods (figs. 8 and 7(b)) vary considerably in appearance. The insufficiently heated areas permitted ice formations to remain on the model and serve as collectors for other ice pieces that would otherwise slide or blow off of the model. In establishing heating levels for marginal de-icing, these ice formations were intentionally ignored, although their presence undoubtedly influenced in varying degrees the aerodynamic removal of ice from adjacent surfaces. This ice also made it difficult to judge when marginal conditions for cyclic operation were attained for the rest of the model. This uncertainty resulted in considerable scatter in the marginal heating values.

In order to permit better visualization and comparison of the various cyclic de-icing results, the succeeding sections will present the marginal de-icing heating rates for various icing and model conditions and also a generalization of parting-strip heat requirements. These two heating requirements will then be combined in the form of an equivalent-continuous heating requirement, which permits direct comparisons of model components and also of anti-icing with de-icing heating requirements.

Marginal de-icing heating rates. - The heating rates for the de-icing portion of the cycle (determined by eq. (1)) are shown in figure 9 as a function of the heat-on period for the three airfoil sections of both model versions. These data are for a total cycle time of about four minutes and cover a wide range of test conditions. The liquid-water content values for these data are presented in either a high or a low range. The low liquid-water-content range extends from approximately 0.3 to 0.7 gram per cubic meter, whereas the high range extends from 0.7 to 1.3 grams per cubic meter.

Effect of datum air temperature. - The variable having the greatest effect on de-icing heat requirements is the datum air temperature, which is presented in figure 10 for a 25-second heat-on period and mean values

of the secondary variables of airspeed, angle of attack, slat position, and liquid-water content. A decrease in the datum air temperature requires a significant increase in heating rate for de-icing with a constant heat-on period; at 0° F, the heating requirements are approximately double those at 25° F. The three airfoil sections shown in figure 10 require approximately the same heating rates. At a datum air temperature of 10° F, the heating requirements range from 16,800 Btu per hour per foot span for the slat to 20,800 Btu per hour per foot span for the standard airfoil.

Effect of parting strips. - The effect of a parting strip on the de-icing heat requirements can be determined from figure 9 by comparing large and small identical symbols. The large symbols denote tests in which the parting strips in the original model were unheated. In general, at high datum air temperatures, the heat requirements for de-icing are nearly independent of whether the parting strips were heated or not heated. At low air temperatures, more heat is required to de-ice the airfoil with unheated than with heated parting strips. This increased heat requirement at lower temperatures appeared more pronounced with the standard airfoil than with the slat.

The effect of parting strips in the present swept model on the overall de-icing heat requirements was on an average less than that in references 1 and 2 for unswept models. A swept airfoil facilitates ice removal by an air velocity component along the span of the leading edge, thereby preventing a balance of the aerodynamic forces on an ice cap over the airfoil nose. In addition, the leading-edge glaze-ice formations are discontinuous in spanwise extent (see fig. 6). This discontinuity permits easy break-up of the ice formation during de-icing and results in removal in small pieces. This latter effect of airfoil sweep is not as evident with rime-ice deposits and may partly explain the increased heating required for de-icing at the low air temperatures when the parting strips are not heated.

The rates of heat flow to the parting strips will be presented in "Parting-strip heat requirements."

Effect of angle of attack and slat position. - For the range of conditions studied, no consistent or pronounced effects on the heat requirements are noted for the slat or standard airfoil (fig. 9), either from changes in airfoil angle of attack or slat position.

Effect of airspeed. - The effect of airspeed on de-icing heat requirements was found to be small over the range studied, partly because of compensating effects of two opposing factors. Whereas higher airspeeds require increased heating to elevate the surface temperature a given amount, higher speeds also increase the aerodynamic forces that remove the ice.

Effect of heat-off (icing) period and liquid-water content. - The effect of the heat-off period on the heat-on period required for de-icing is shown in figure 11 for the low range of liquid-water content. Each curve in figure 11 represents conditions of constant airspeed, air temperature, angle of attack, liquid-water content, and heating rate. An increase of 1 minute in the heat-off period generally requires an increase in the heat-on period of between 1 and  $1\frac{1}{2}$  seconds. However, in the case of the standard airfoil at 260-mph airspeed, the increase was unaccountably about double that of the other cases. The increased heat-off periods allow the supply ducts and model interior to cool down nearer to the ambient temperature and largely explain the increased heating time requirement for de-icing.

The effect of the heat-off period as shown in figure 11 is comparable to that determined in reference 1, in which the heat-off period was varied through a range from 4 to 11 minutes. However, in reference 1 an increase in the liquid-water content (other factors constant) required a slight increase in the heat-on time, whereas in the present investigation no significant trends with liquid-water content are evident.

Comparison of airfoil models. - The de-icing heating rates required for the modified model were less than those required for the original model; the two versions of the standard-airfoil section compared most closely (fig. 9(a)). These reductions in heating rate were caused in part by reduced heated areas in the modified model and will be discussed later.

The standard-airfoil section is somewhat similar in construction to the 12-percent-thick airfoil in references 1 and 2. Differences in size, gas supply system, and test conditions prevent a direct comparison between these airfoils. However, the de-icing heat requirements for the standard-airfoil section appear to be slightly greater than those of the 12-percent-thick airfoil of reference 2.

Parting-strip heat requirements. - The parting-strip heat requirements are shown in figure 12 as functions of datum air temperature and airspeed for both the gas and electrically heated parting strips of the original model. The heat requirements are approximately linear with air temperature. The data in figure 12 cover the whole range of operation of the two parting-strip heat supplies, and the curves are drawn to represent mean values. The standard-airfoil parting strip, for example, required approximately 530 and 450 Btu/(hr)(ft span), respectively, for 260- and 175-mph airspeed and 30°-F temperature differential.

The ice-free width of both parting strips varied with operating conditions and icing period from approximately 3 inches to  $1\frac{1}{2}$  inch; the greater widths occurring at the higher air temperatures. The gas-heated parting-strip requirements are compared in figure 12(a) with

those of the gas-heated parting strip of reference 2 for an ice-free width of about  $1\frac{1}{2}$  inches. The parting strip of reference 2 required about 30 percent less heat flow mainly because of less chordwise thermal conduction in the thinner outer skin of the airfoil. The electric parting strip on the slat (fig. 12(b)) at the higher datum air temperature required slightly less heat than the gas-heated parting strip because of less conduction in the structure and better heating control. At low air temperatures, the two types of parting strips required nearly equivalent heating.

The foregoing hot-gas parting-strip heat requirements (fig. 12(a)) are based on the spanwise drop in duct gas temperature per foot span. In this short-span model, no account is taken of the heat left in the gas at discharge from the parting-strip duct. This heat should be considered in a full-scale design, as it also must be applied by the heat source. Consequently, more input heat flow is required in a full-span design than is indicated in figure 12. Since the heat wasted at discharge is affected by the operating levels of gas temperature and flow, these factors have been correlated with the spanwise drop in gas temperature for use in the design of similar gas-heated parting strips (fig. 13). The correlation is obtained by plotting the ratio of the spanwise gas temperature drop per foot span  $\Delta t_g/\Delta L$  to the differential temperature between the parting-strip inlet gas and datum air ( $t_{g,i} - t_d$ ) as a function of parting-strip gas flow where

$t_g$  parting-strip gas temperature, °F

$L$  parting-strip span, ft

$t_{g,i}$  parting-strip inlet gas temperature, °F

$t_d$  datum air temperature, °F

Figure 13 includes all the data obtained during this investigation of a gas-heated parting strip, and the liquid-water content ranges are the same as in figure 9.

As an example, one approach to the parting-strip design problem is to determine the minimum levels of gas temperature and flow that will allow a fin construction to conduct heat to the parting strip in the amounts dictated by figure 12 (and figs. 13 and 14 of ref. 2). These levels can then be assigned to the parting-strip exit. Using figure 13 and figure 9 of reference 2 for the gas flows and temperature assigned, the gas temperature drop per foot span may be estimated. For a long duct, several segments should be assigned, and for each segment, figure

13 should be used and the fin design altered to account for the increasing gas temperature with distance toward the inlet. The inlet gas temperature is then used to calculate the parting-strip heat-source requirement.

Equivalent-continuous heating rates. - As stated previously, the equivalent-continuous heating rate is defined as the heating rate required for de-icing divided by the cycle ratio, with the parting-strip heating rate (continuous) added whenever heated parting strips are used. This definition of heating requirements is analogous to a steady-state heat-source demand and permits a direct comparison between anti-icing and cyclic de-icing heat requirements.

The equivalent-continuous heating requirements per foot span for the three airfoil sections of both model versions are shown in figure 14 as a function of the cycle ratio. Anti-icing corresponds to a cycle ratio of 1.0 (continuous heating). The cyclic de-icing heat requirements with cycle ratios greater than 6 (fig. 14) are only a fraction of the anti-icing requirements. The anti-icing heat requirements, defined in CONDITIONS AND PROCEDURES, vary almost directly with airspeed and liquid-water content, whereas for the cyclic de-icing heat requirements, these two variables are of secondary importance. The greatest proportionate reduction in heat requirement between anti-icing and de-icing, therefore, occurs at high values of liquid-water content and airspeed. For the conditions shown in figure 14, the de-icing heat requirement for the original model averages about 25 percent of the anti-icing heat requirement, and for the modified model (dashed lines) the requirement is even less. The heat requirement for the slat is nearly constant for cycle ratios between 8 and 26, whereas for the standard and fixed airfoils the heat requirement decreases slightly as cycle ratio increases. For design purposes, selection may be made from a wide range of cycle ratios for a given heat-source capacity with nearly the same de-icing performance.

In general, the equivalent-continuous heat requirement data of figure 14 follow the trends discussed for the data of figure 9 (de-icing heating rate). In figure 14, the parting-strip heat requirements have been included in the ordinates and, compared with figure 9, cause a slight increase in the heat requirements for the heated parting-strip cases relative to the cases with unheated parting strips. The modified model (without parting strips) required an average of about 60 percent as much heat-source capacity as the original model using heated parting strips. The unswept airfoil of references 1 and 2 using heated parting strips required total heating rates between those for the original and modified models used in this study.

Comparison of anti-icing and de-icing. - The designer of ice-protection systems is often confronted with the problem of selecting between anti-icing and de-icing heating systems. De-icing requires

3081

much less heat than anti-icing but allows some amount of ice to form on the airfoil. If, however, some runback ice may be tolerated, then submarginal anti-icing might appear attractive as a means of lowering the heating requirement below that for complete anti-icing without the complexity of a cyclic de-icing system. As heat flow rates are reduced below the anti-icing level, small amounts of runback ice begin to accrue. As heating levels are further reduced, the resulting ice formations appear progressively farther forward toward the leading edge and form flow-disrupting spanwise ridges. It is thus necessary to compare these two methods of heating in terms of airfoil drag due to the resulting ice formations as well as by their over-all system heat requirements.

A comparison of the heat-source capacities required for cyclic de-icing and anti-icing systems is shown in figure 15. For the original and modified cyclic de-icing systems, the marginal heat requirement data of figure 14 for a cycle ratio of 12 are presented in figure 15 as a function of the datum air temperature for a speed of about 260 mph. Two curves are also shown for anti-icing (continuous heating of the original model); the higher representing ice-free anti-icing, while the lower curve represents an arbitrary reduction to approximately 55 percent of the heating rate of the anti-icing condition.

With this submarginal anti-icing, ice formations build up on the subfreezing areas of the model as shown in figures 16(a) and (b). For comparison, photographs of a marginal cyclic de-icing condition are also shown (fig. 16(c)). The resultant runback ice formations after 6 to 9 minutes of submarginal anti-icing form spanwise ridges near the leading edge (figs. 16(a) and 16(b)). These ice formations will appreciably increase the drag of the airfoil and also may impair the lift. The cyclically de-iced airfoil, requiring only about 40 percent as much heat flow as the submarginal anti-icing example, is completely free of ice over the entire heated leading-edge area after each heating period (fig. 16(c)). During the icing phase of the cycle, ice will deposit on the airfoil leading edge as shown in figure 8, but is restricted to a small size by the short duration of the icing period.

The effects of ice formations on the drag of airfoils are presented in references 3, 5, 6, and 7. In addition, comparison of airfoil drag values as affected by de-icing and submarginal anti-icing systems is given in figure 24 of reference 5. From this comparison and the additional information in this investigation (figs. 15 and 16), it is concluded that as anti-icing heating rates are lowered toward the cyclic de-icing heating values, the resultant airfoil drags for the two cases are equivalent after a short time in icing (one or two cycles of the de-icing system), and thereafter, the submarginal anti-icing system will always contribute more drag.

## Local and Internal Heat-Transfer Processes

The following properties of the gas-heating system will now be presented: surface temperature variations, gas temperature variations, and ice-shedding characteristics. These data were obtained during marginal de-icing operation of the heating system.

Surface temperature variations. - The variation of surface temperature with time is shown for several thermocouple locations in figures 17, 18, and 19(a). The operating conditions for these curves are listed in table I. In figure 17, four representative temperature curves show the typical heating and cooling portions of the surface temperature history. The peaks of the temperature curves represent very closely the points at which heat flow was turned off. The time at which shedding of ice occurs is also shown. Large variations in the temperatures and times of ice-shed and the peak surface temperatures were obtained.

The general shape of all of the temperature-time curves shown concurrently for six lower surface thermocouples is about the same (fig. 18). The temperature curves for thermocouple locations farther from the leading edge peak at lower temperatures because of cooling of the gas flow in the passages. The ice-shedding points also indicate shedding at lower temperatures at positions farther from the leading edge. This trend results from the nature of the ice deposit toward the rear of the impingement area. Here, because the ice forms in small isolated particles, the formations shed more easily and more nearly at a surface temperature of 32° F than do the large, thick leading-edge ice formations.

Comparisons of surface temperatures measured at the midpoints of the double-skin gas passages with those measured at the rivet lines are also shown in figure 18. Near the leading edge, the temperature at the rivet line rises above that for the passage midpoint, probably because of thermal conduction from the D-duct through the skins and stiffeners. Farther aft from the leading edge where little internal conduction occurs, the rivet-line temperature lags behind the midpassage surface temperature.

A comparison of surface temperatures in dry air and icing conditions for the modified model is shown in figure 19 for similar heating and air-flow conditions. At the leading edge (fig. 19(a)), the surface temperature in icing reached a higher value throughout the heating period than that in dry air, possibly because the thick ice cap, prior to its removal, shielded the surface from the cooling effect of the air flow. Elsewhere over the heated area, as shown in figure 19(b), the temperatures in icing tended to be less than those in dry air, especially in the impingement zone. The variation of surface temperature is shown for only the peak values of the time curves (approx. at point of heat-off). The upper surface shows little difference between icing or dry air conditions (practically no impingement at 4° angle of attack), whereas on the lower surface, the temperatures were appreciably lower in the icing condition as a result of the droplet impingement effects.

**CONFIDENTIAL**

The surface temperature variations for the original standard airfoil and slat are compiled in figure 20 at various time increments during their heating periods. These data show that at any given time, surface temperatures for such cyclic gas-heating systems tend to be undesirably nonuniform. The temperature pattern over the original slat surface was characterized by elevated temperatures over the D-duct area and relatively low temperatures over the rest of the surface. The lower-surface trailing lip lagged in temperature rise because of the circuitous path taken by the hot gas. (This lip area received heat by conduction from the D-duct and by the gas flow from the rear face.) Some of the surface temperature gradients during the heating period shown in figure 20 exceed 100° F per inch of distance. This nonuniformity of surface temperature causes ice formations to adhere to subfreezing surfaces while adjacent parts of the ice are needlessly melted away. Simultaneous melting of all of the ice bond requires uniform surface temperatures during the heating period which, as shown in figure 20, are difficult to obtain in a practical construction.

The minimum width of the ice-free area, or parting strip, can be seen in figure 20 from the curve for zero heating time as the distance along the surface that is above 32° F (see example in fig. 20(a)). For heat economy as well as reliable de-icing, it is desirable to have narrow parting strips. In order to accomplish this, the conduction of heat away from the parting-strip fin in the outer skin should be low, resulting in steep temperature gradients on either side of the fin attachment point. These regions near the fin in the standard airfoil were sometimes slow in shedding ice. This local heating deficiency was not due to the parting-strip design as such, but rather to the heating arrangement for cyclic de-icing. These areas were not heated sufficiently by the internal gas flow, because the entrances to the upper- and lower-surface double-skin flow passages were too far from the parting-strip fin and thus too far apart. The remedy is to extend the inner skins closer to the parting-strip fin without making thermal contact with either the fin or the outer skin.

Gas temperature variations. - The temperature loss or lag in the supply lines and distribution ducts is significant to the design and performance of a hot-gas cyclic de-icing system. The amount of temperature drop throughout the slat and standard-airfoil gas supply systems may be seen in figure 21 together with the resulting surface temperature profiles. The gas temperature at the cycling valve was maintained constant (420° to 460° F) whereas the other temperatures in figure 21 increased with time during the heat-on period to the peak values shown. The temperatures are plotted in terms of the developed lengths of flow channel and surface. This plotting permits visualization of the temperature loss through the system. The D-duct temperature gradients exceeded those in the supply ducts but were less than those in the double-skin heating passages. The surface temperatures were measured in the main instrumentation planes (fig. 1(b)), which are normal to the leading-edge

**CONFIDENTIAL**

3081

CC-3

D-ducts at the points shown in figure 21. The gas temperatures were measured in the instrumentation plane for the standard airfoil but along the foremost spanwise heating passage for the slat.

For the standard airfoil (fig. 21(a)), the temperature losses in the supply ducts for the original and modified models were quite large. For example, the gas temperature at the D-duct instrumentation plane (modified model) was only 57 percent (based on temperature differentials above the datum temperature) of the temperature available at the cycling valve at the end of the heat-on period, and was only 78 percent as high when the flow was maintained until ultimate levels were stabilized.

The D-duct temperatures in the modified model showed a temperature gradient less than half that for the original model; the increased D-duct insulation and the absence of a parting-strip duct in the modified model helped to account for this improvement.

The surface temperatures for the modified standard airfoil are more uniform and considerably below those for the original model. This greater uniformity resulted from removal of parting strips, added insulation, and better adjustment of flow distribution. The difference in surface temperature levels resulted, in part, from the instrumentation plane on the modified model which appeared to run colder than the rest of the airfoil section, as shown by the incomplete ice removal in figure 7(b).

For the slat (fig. 21(b)), the supply duct for the modified model shows a reduction in temperature loss over the standard airfoil ( $112^{\circ}$  F in 65 in. of duct length compared with  $164^{\circ}$  for the standard airfoil with 63 percent more gas flow). This reduction was due to more complete insulation of the slat supply duct. The modified-slat D-duct showed a marked decrease in temperature gradient over the original slat, as was the case for the standard airfoil. A more uniform and lower surface temperature pattern also resulted with the modified version of the slat.

Ice-shedding characteristics. - The observed time of ice-shedding from some of the thermocouple locations on the lower surface of the original model during de-icing is given in table II. The shedding time is tabulated against de-icing heating rate and surface temperature at the time of shedding, although the shedding temperature was rather random for locations near the leading edge. The ice-shedding time was found to increase as the heating rate decreased. Data from table II, shown in figure 22 for one operating condition, indicate that ice-shedding characteristics may be consistent for a given component but may differ for other components. The ice-shedding curves for the slat have the same shape as those for the standard airfoil, but are spaced differently with respect to surface location because of differences in internal heating arrangements. A general correlation of ice-shedding factors might be possible on the basis of localized surface heat-transfer rates if these were known.

The heating time required to shed ice is compared in figure 23 with the time required to reach a surface temperature of 32° F for the standard-airfoil section. The heated lower surface tends to shed ice at the rear-most locations at the time the surface temperature reaches 32° F. Near the leading edge, the surface reaches 32° F several seconds before ice-shedding occurs. These trends were also evident in the data of reference 2. As the heating rates were increased for a particular icing condition (e.g., up to 30,000 Btu/(hr)(ft span), (fig. 22)), the ice would tend to shed at nearly the same time from the whole lower surface.

#### SUMMARY OF RESULTS

Heating requirements for satisfactory cyclic de-icing were obtained over a wide range of icing and operating conditions for a slat and a standard-airfoil section with and without leading-edge ice-free parting strips. For the models and conditions studied, the following principal results were obtained:

1. Cyclic de-icing was compared with anti-icing and found to require about 25 percent or less of the heat source required for complete anti-icing.
2. De-icing heat requirements were approximately the same with either heated or unheated parting strips. This resulted from the spanwise flow component associated with swept wings, which helped remove ice by blowing parallel to the leading edge and which also caused leading-edge glaze ice to form in discontinuous spanwise saw-tooth pieces that broke up and shed readily without need of a parting strip.
3. Cyclic de-icing heat requirements increase markedly with decrease in the datum air temperature. Negligible or inconsistent effects on heat requirements were found for the following variables: angle of attack, slat position, airspeed, and liquid-water content. An increase in heating rates was required with an increase in the icing period of the cycle.
4. The heating time required to shed ice formations near the leading edge was several seconds longer than that required to elevate the surface temperatures to 32° F. Toward the aft end of the heated area, the ice shed when surface temperatures were close to 32° F. At high rates of heating, the ice would tend to shed almost simultaneously over the whole heated lower surface of the standard airfoil.
5. Several localized areas of the model were extremely slow in shedding ice because of insufficient heating at these points. Most of these deficiencies were attributed to the structural complexity inherent with leading-edge slats and illustrate the need for providing uniform surface-temperatures over the model during the heating period.

6. The modified version of the model, without parting strips and with improved insulation and flow distribution, required less heat-source capacity than the original version by about 40 percent. The cyclic heat-source requirements of the unswept gas-heated, 12-percent-thick airfoil of reference 2 were approximately between the requirements of the present original and modified models. More uniform surface-temperatures and smaller D-duct gas-temperature losses were obtained with the modified model than with the original version.

Lewis Flight Propulsion Laboratory  
National Advisory Committee for Aeronautics  
Cleveland, Ohio, February 23, 1956

#### REFERENCES

1. Gray, V. H., Bowden, D. T., and von Glahn, U.: Preliminary Results of Cyclical De-Icing of a Gas-Heated Airfoil. NACA RM E51J29, 1952.
2. Gray, Vernon H., and Bowden, Dean T.: Comparison of Several Methods of Cyclic De-Icing of a Gas-Heated Airfoil. NACA RM E53C27, 1953.
3. Bowden, Dean T.: Investigation of Porous Gas-Heated Leading-Edge Section for Icing Protection of a Delta Wing. NACA RM E54I03, 1955.
4. Gray, Vernon H., and Bowden, Dean T.: Icing Characteristics and Anti-Icing Heat Requirements for Hollow and Internally Modified Gas-Heated Inlet Guide Vanes. NACA RM E50I08, 1950.
5. von Glahn, Uwe H., and Gray, Vernon H.: Effect of Ice Formations on Section Drag of Swept NACA 63A-009 Airfoil with Partial-Span Leading-Edge Slat for Various Modes of Thermal Ice Protection. NACA RM E53J30, 1954.
6. Gray, Vernon H., and von Glahn, Uwe H.: Effect of Ice and Frost Formations on Drag of NACA 65<sub>1</sub>-212 Airfoil for Various Modes of Thermal Ice Protection. NACA TN 2962, 1953.
7. Bowden, Dean T.: Effect of Pneumatic De-Icers and Ice Formations on Aerodynamic Characteristics of an Airfoil. NACA TN 3564, 1956.

TABLE I. - CONDITIONS FOR FIGURES 17 TO 19

Curve	Figure	Model	Airfoil section	Surface	Distance from leading edge, in.	Airspeed, mph	Datum air temp., °F	Liquid-water content, gm/cu m	Angle of attack, deg	Slat position	Parting strip	De-icing heating rate, Btu/(hr) (ft span)	Cycle ratio	Comments
a	17	Modified Original	Slat	Lower	1.5	175	0	0.4	4	Closed	None	20,200	17	-----
b			Standard		8.5	175	10	.6	8	Half out	Gas heated	31,000	19.5	-----
c			Fixed		7.3	260	25	.8	4	Closed	Electric	22,500	24.5	-----
d			Slat		1.5	175	10	.6	8	Half out	Electric	12,500	8.1	-----
e	18	Original	Standard	Lower	1.9	260	10	.5	4	Closed	Unheated	29,950	10.2	-----
f					8.5									-----
g					15.5									-----
h	19	Modified	Standard	Leading edge	0	260	10	.3	4	Closed	None	31,820	25.0	Icing conditions
i					0									260

TABLE II. - ICE-RELEASE DATA

Airfoil	Distance from leading edge, in.	Heating time to shed ice, sec	Temperature at ice-shed, °F	Heating rate, Btu/(hr)(ft span)	Time for surface to reach 32° F, sec	Airspeed, mph	Datum air temp., °F	Angle of attack, deg	Slat position	Parting strip
Standard	1.9	5	54	28,600	1.5	175	10	8	Half out	Heated
		4	50	27,850	1.5	175	10	12	Out	Heated
		3.5	53	22,300	1.5	260	25	2	In	Heated
		4.5	53	20,400	1.5	260	25	2	In	Heated
		6	45	20,400	2.5	260	25	0	In	Unheated
		7	50	20,500	4	175	10	8	Half out	Unheated
		7	68	29,950	3	260	10	4	In	Unheated
		3	51	28,250	0	260	25	4	In	Unheated
		6	46	24,400	1	175	25	8	Half out	Unheated
		13	63	15,700	1	175	25	8	Half out	Unheated
		8	66	23,500	2.5	260	10	4	In	Heated
		5	57	24,200	1.5	175	10	8	Half out	Heated
		4	57	24,700	1.5	260	25	0	In	Heated
		8	60	24,600	2	260	25	0	In	Unheated
		4	54	23,700	1	260	25	4	In	Heated
		5	58	24,000	1.5	260	25	4	In	Heated
	6	49	20,900	2	175	10	8	Half out	Heated	
	5	55	31,000	2	175	10	8	Half out	Heated	
	5.2	7	35	28,600	4	175	10	8	Half out	Heated
		7	32	27,850	7	175	10	12	Out	Heated
		10	40	20,500	5	175	10	8	Half out	Unheated
		6	39	29,950	3.5	260	10	4	In	Unheated
		2	40	28,250	.5	260	25	4	In	Unheated
		3.5	32	24,700	3.5	260	25	0	In	Heated
		5	40	23,700	2	260	25	4	In	Heated
	8.5	7	28	28,600	8	175	10	8	Half out	Heated
		7	28	27,850	8	175	10	12	Out	Heated

TABLE II. - Continued. ICE-RELEASE DATA

Airfoil	Distance from leading edge, in.	Heating time to shed ice, sec	Temperature at ice-shed, °F	Heating rate, Btu/(hr)(ft span)	Time for surface to reach 32° F, sec	Airspeed, mph	Datum air temp., °F	Angle of attack, deg	Slat position	Parting strip
Standard	8.5	6	32	22,300	6	260	25	2	In	Heated
		7	30	20,400	.7	260	25	2	In	Heated
		12	33	20,500	11.5	175	10	8	Half out	Unheated
		8.5	36	29,950	7.5	260	10	4	In	Unheated
		2	30	28,250	3	260	25	4	In	Unheated
		6	28	24,400	7	175	25	8	Half-out	Unheated
		6	34	24,700	5	260	25	0	In	Heated
		5	32	23,700	5	260	25	4	In	Heated
	12.1	12.5	31	20,500	13	175	10	8	Half out	Unheated
		11	31	29,950	12	260	10	4	In	Unheated
		5	31	24,700	5.5	260	25	0	In	Heated
		5.5	31	23,700	5.5	260	25	4	In	Heated
	15.5	9	36	22,300	3	260	25	2	In	Heated
		5	31	20,400	5	260	25	2	In	Heated
		16	34	20,500	15	175	10	8	Half out	Unheated
		12	31	29,950	12.5	260	10	4	In	Unheated
		4.5	31	28,250	5	260	25	4	In	Unheated
		5	30	24,700	5	260	25	0	In	Heated
		17	38	20,900	14	175	10	8	Half out	Heated
		8.5	33	25,500	8	175	10	8	Half out	Heated
	Slat	1.5	7	51	24,100	1.5	175	10	12	Out
3			53	23,500	1	260	25	2	In	Heated
8			54	14,300	1.5	175	10	8	Half out	Unheated
7			58	26,350	1.5	260	10	4	In	Unheated
3.5			58	24,350	.25	260	25	4	In	Unheated
4.5			44	24,150	1.5	260	10	4	In	Heated
2			40	19,000	1	175	10	8	Half-out	Heated

TABLE II. - Concluded. ICE-RELEASE DATA

Airfoil	Distance from leading edge, in.	Heating time to shed ice, sec	Temperature at ice-shed, °F	Heating rate, Btu/(hr) (ft span)	Time for surface to reach 32° F, sec	Airspeed, mph	Datum air temp., °F	Angle of attack, deg	Slat position	Parting strip
Slat	1.5	1.5	47	25,900	0.5	260	25	0	In	Heated
		3.5	55	25,500	1	260	25	0	In	Unheated
		1.5	50	25,600	0	260	25	4	In	Heated
		6	44	12,500	2.5	175	10	8	Half out	Heated
	3.9	25	29	24,100	29	175	10	12	Out	Heated
		25.5	31	14,300	27	175	10	8	Half out	Unheated
		20	32	26,350	20	260	10	4	In	Unheated
		7	33	24,450	3.5	260	25	4	In	Unheated
		16	33	24,150	15	260	10	4	In	Heated
		13	30	19,000	15	175	10	8	Half out	Heated
		8	38	25,600	.1	260	25	4	In	Heated

CONFIDENTIAL

CONFIDENTIAL

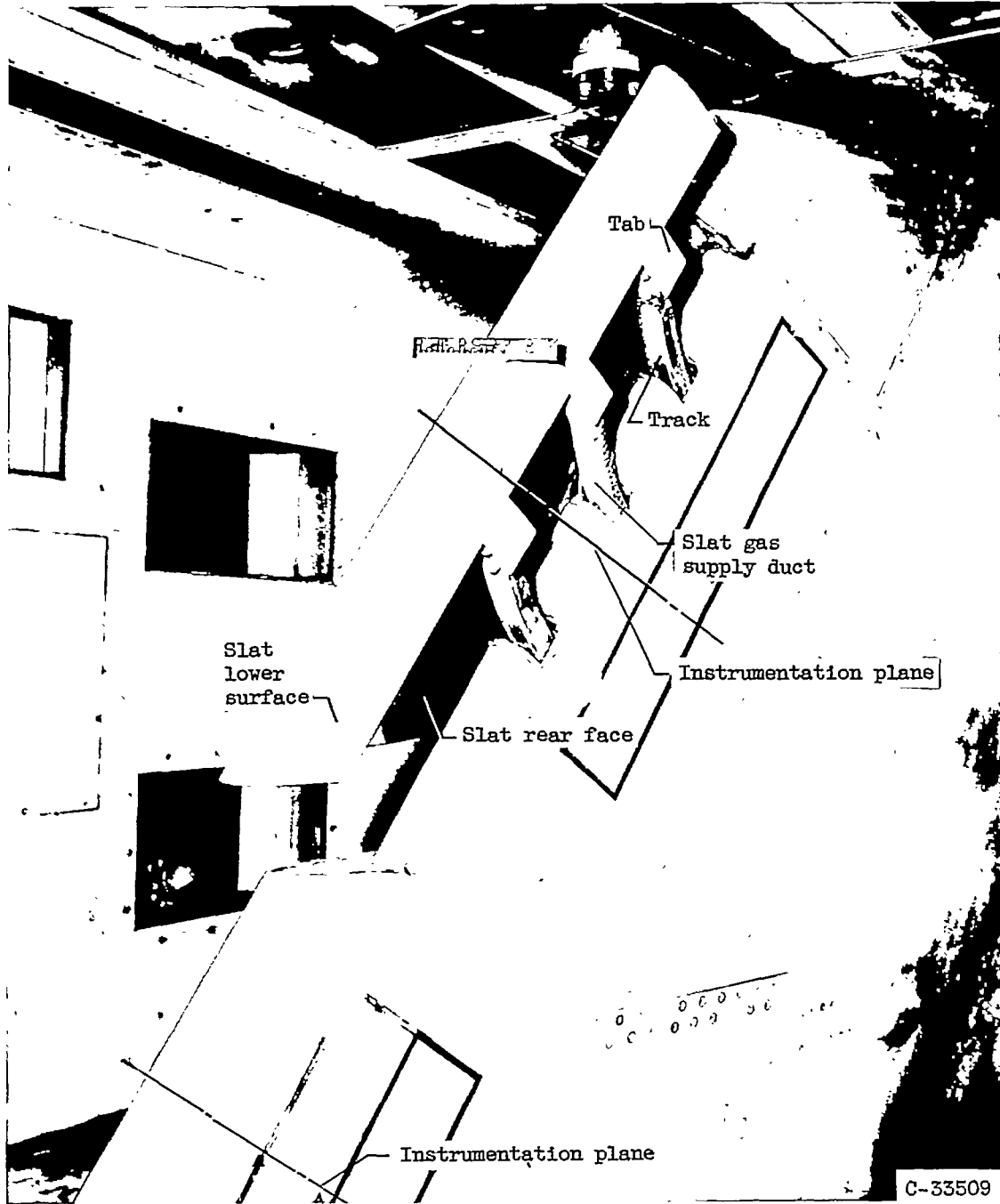
3081

CC-4



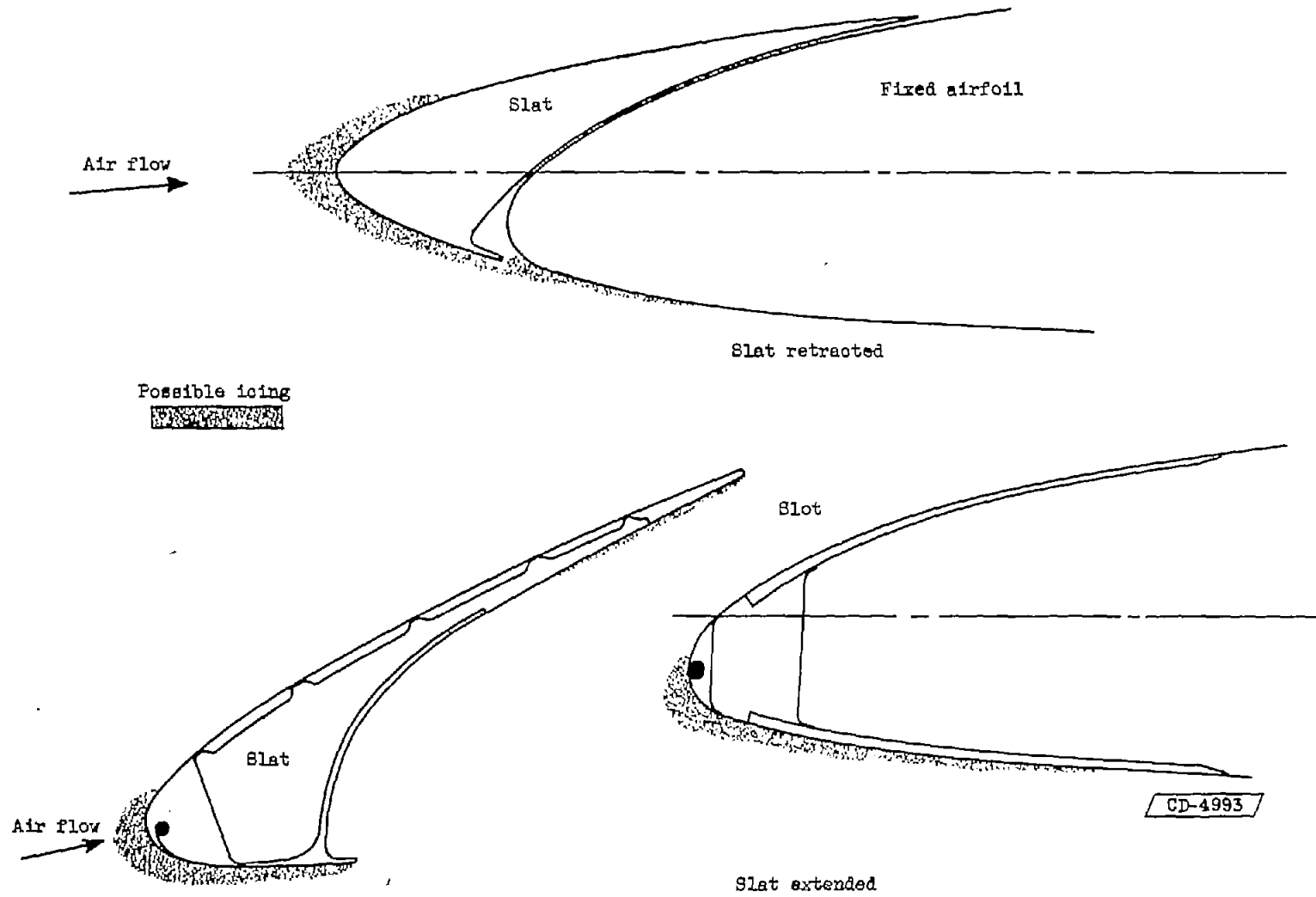
(a) Upper surface.

Figure 1. - Installation of swept airfoil with partial-span leading-edge slat in icing tunnel.



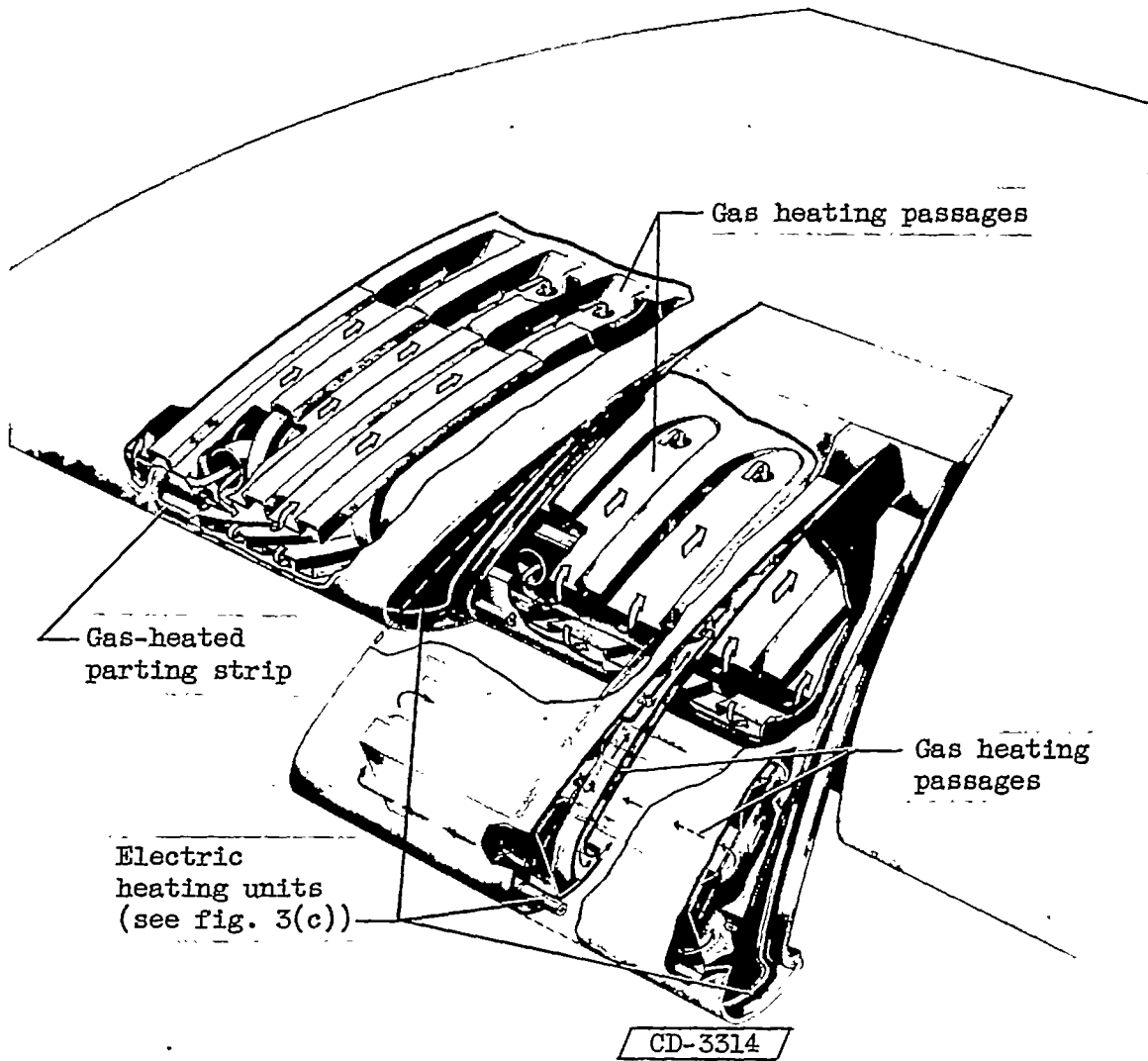
(b) Lower surface.

Figure 1. - Concluded. Installation of swept airfoil with partial-span leading-edge slat in icing tunnel.



(a) Section through slat.

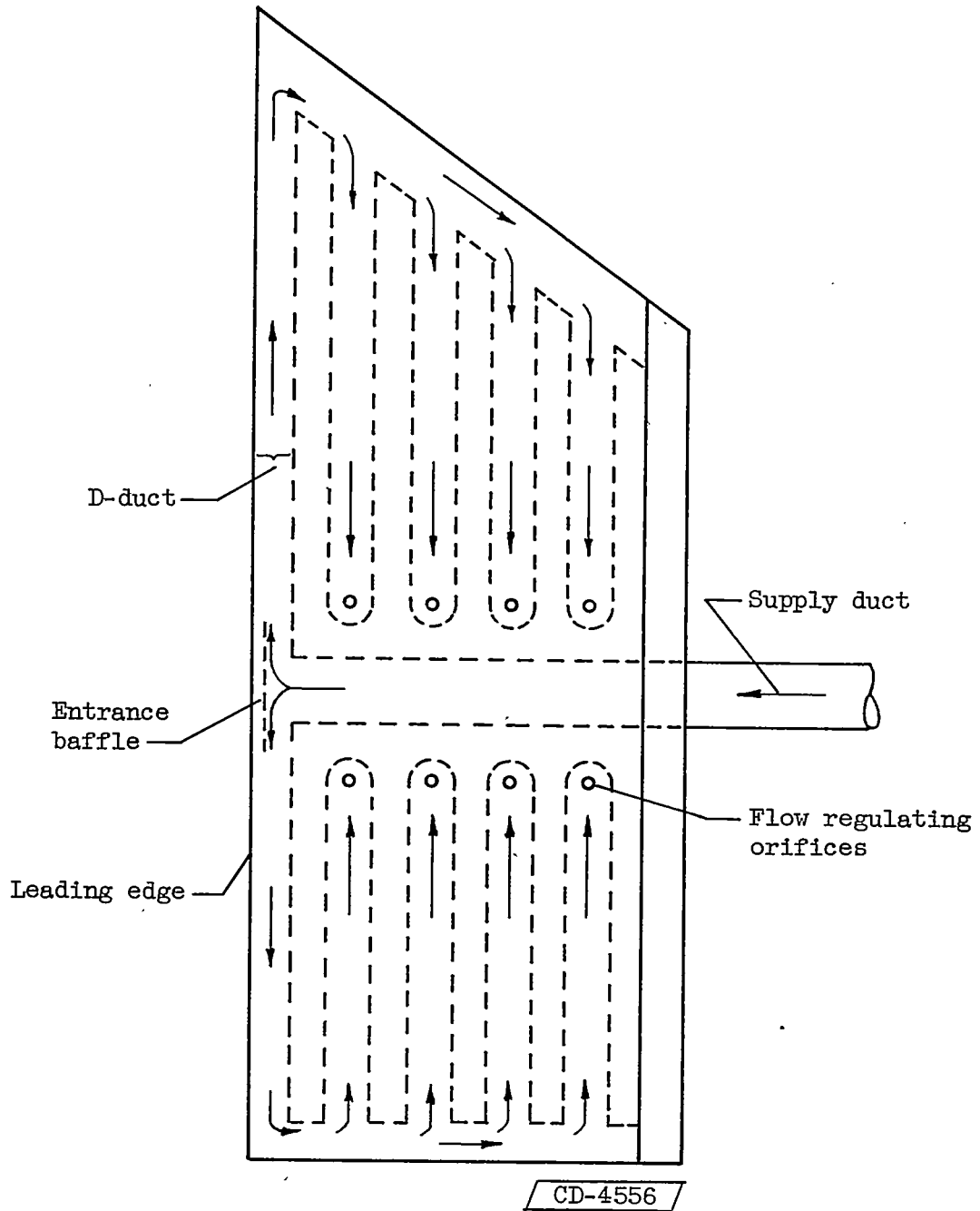
Figure 2. - Relation of main components of model.



(b) Cutaway drawing of model showing heating passages.

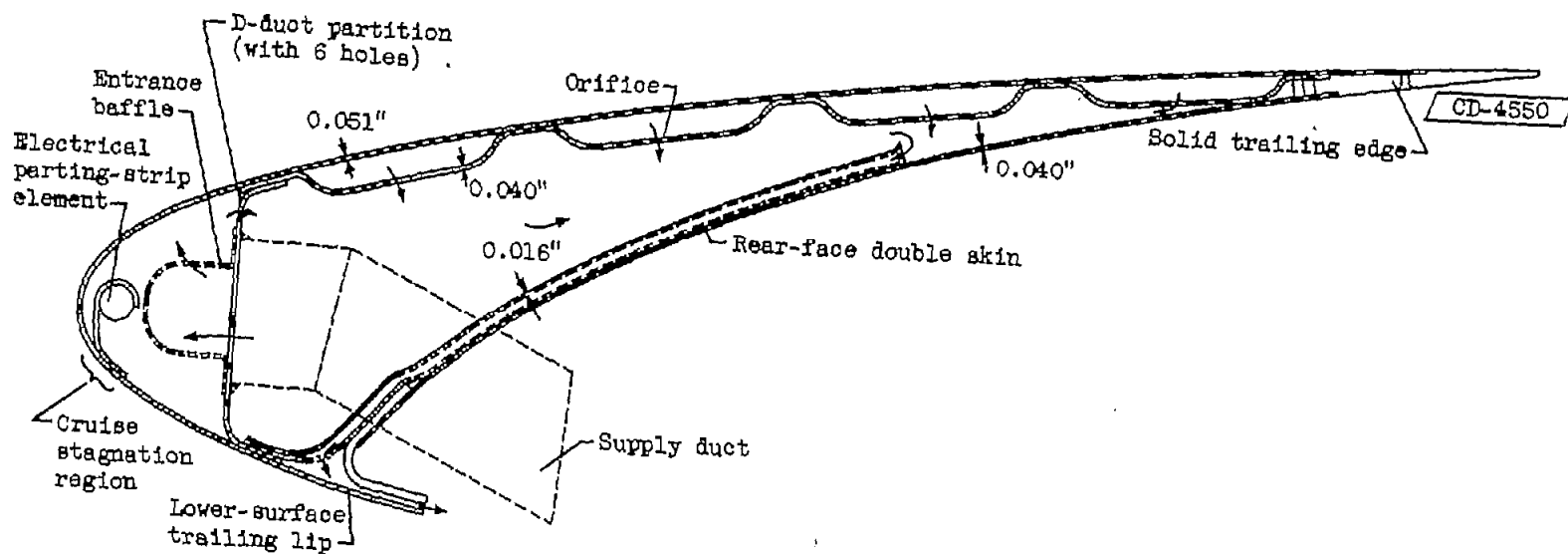
Figure 2. - Concluded. Relation of main components of model.

3081

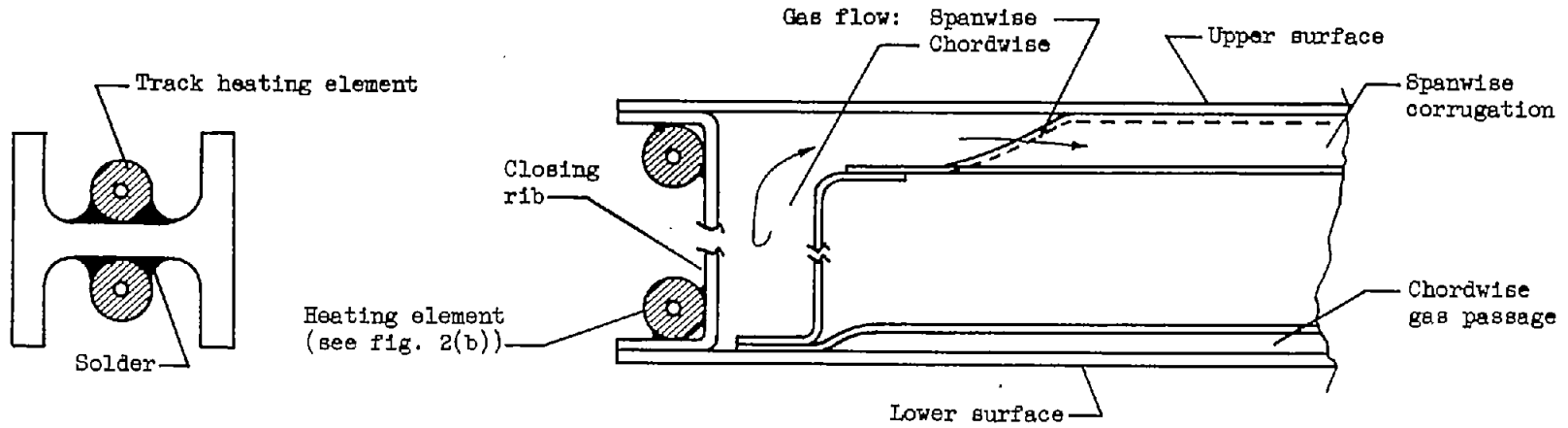


(a) Plan view of heating circuit (original version, upper surface).

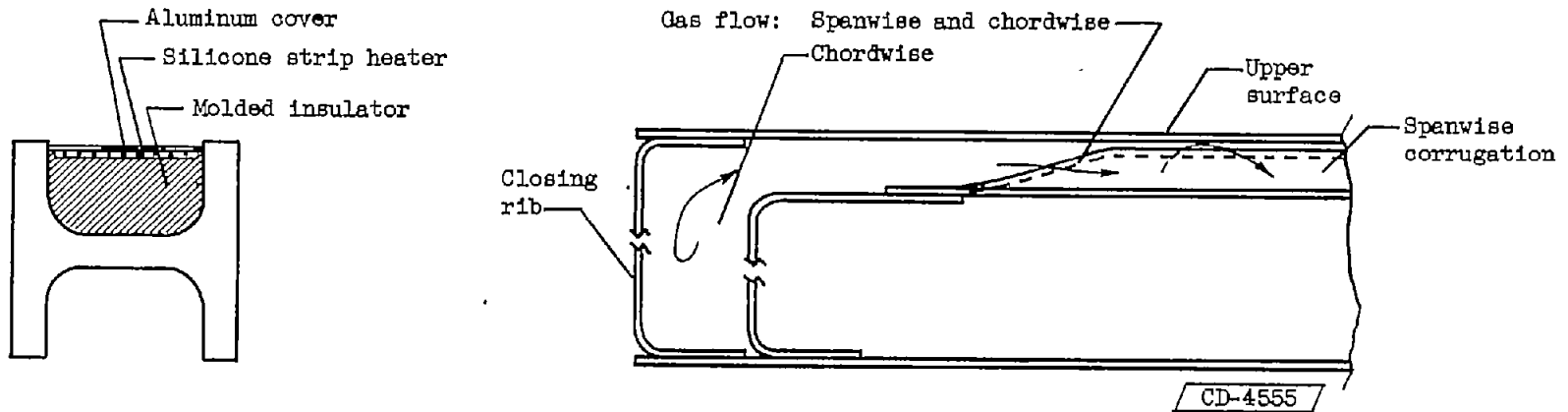
Figure 3. - Slat heating system.



(b) Typical cross section (original version).  
 Figure 3. - Continued. Slat heating system.

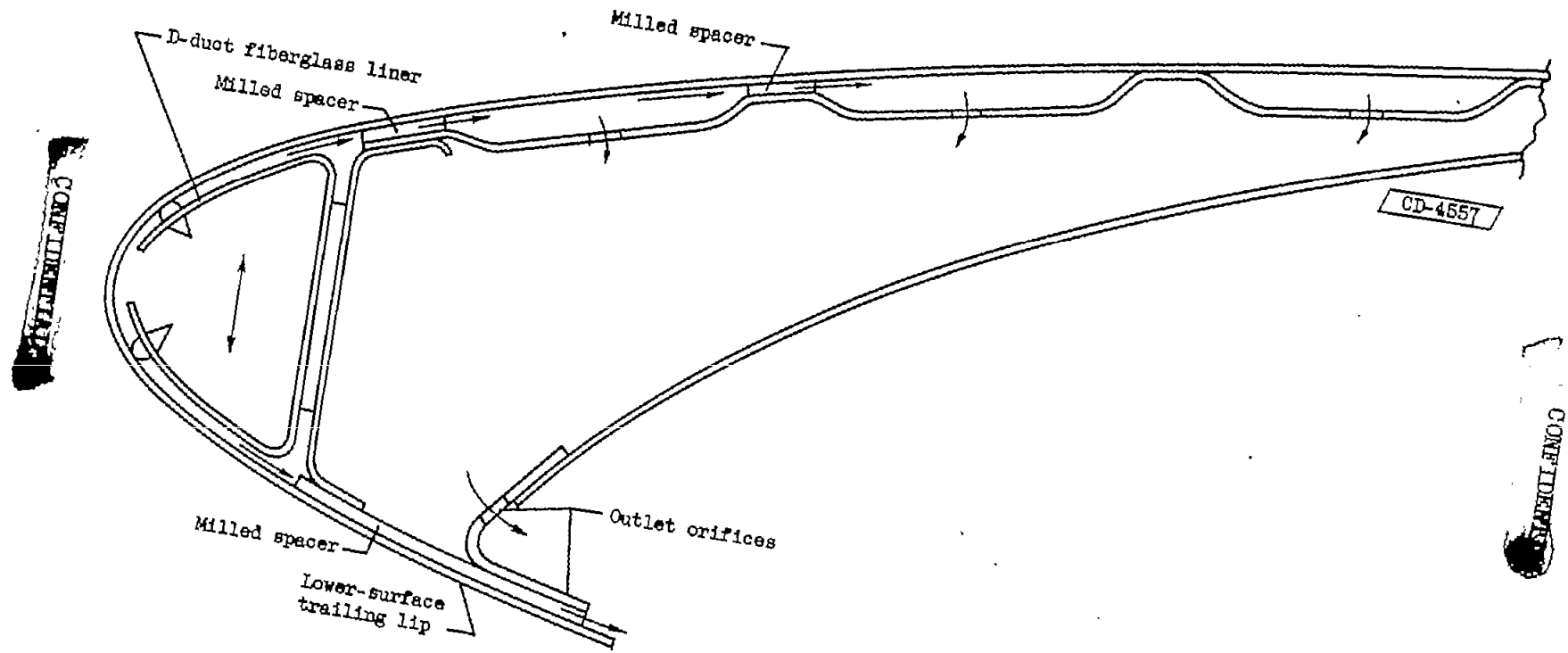


(c) Typical spanwise cross section of track and end of slat (original version).



(d) Typical spanwise cross section of track and end of slat (modified version).

Figure 3. - Continued. Slat heating system.

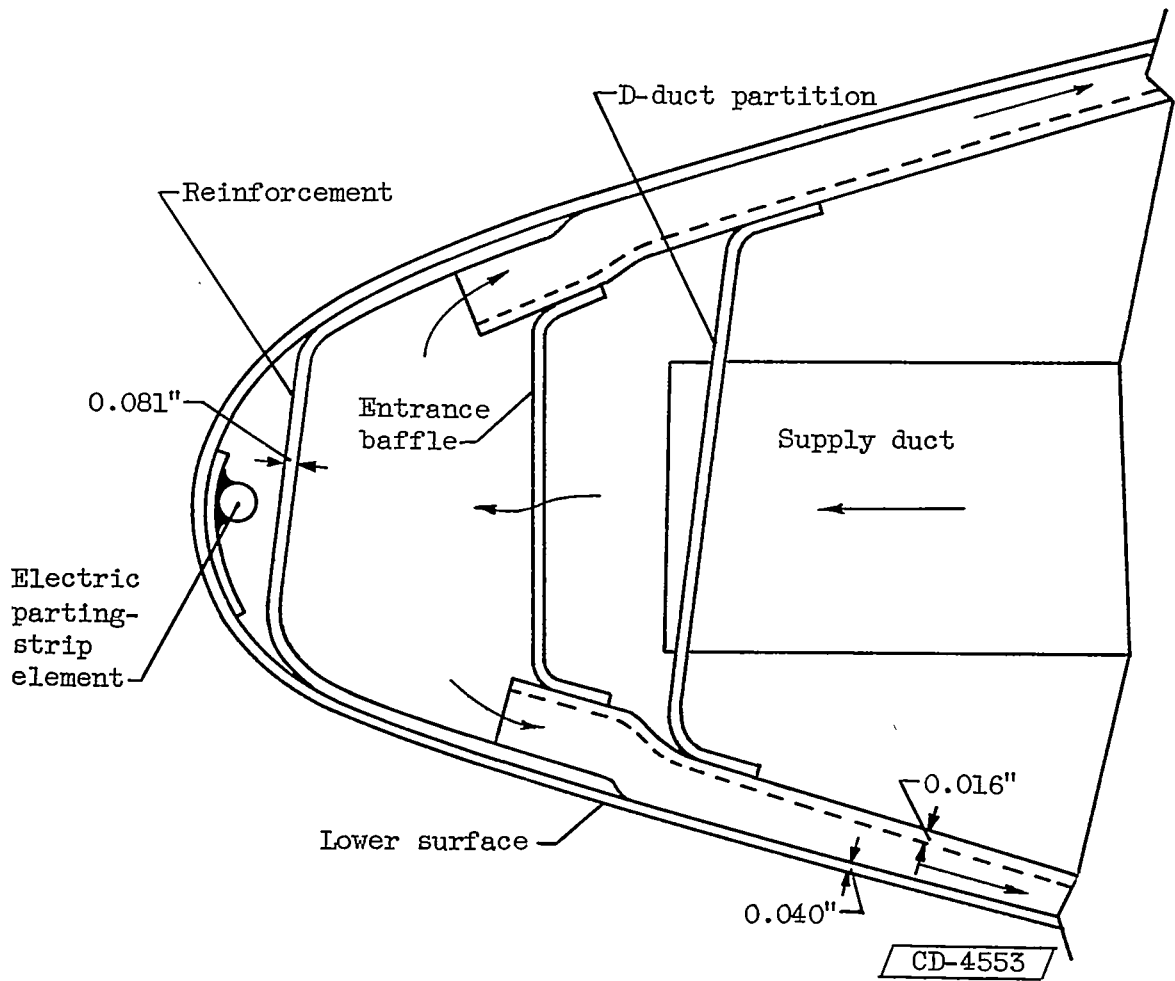


(e) Typical cross section (modified version).  
 Figure 3. - Concluded. Slat heating system.

NACA RM 1156B23

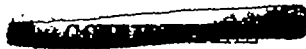
3081

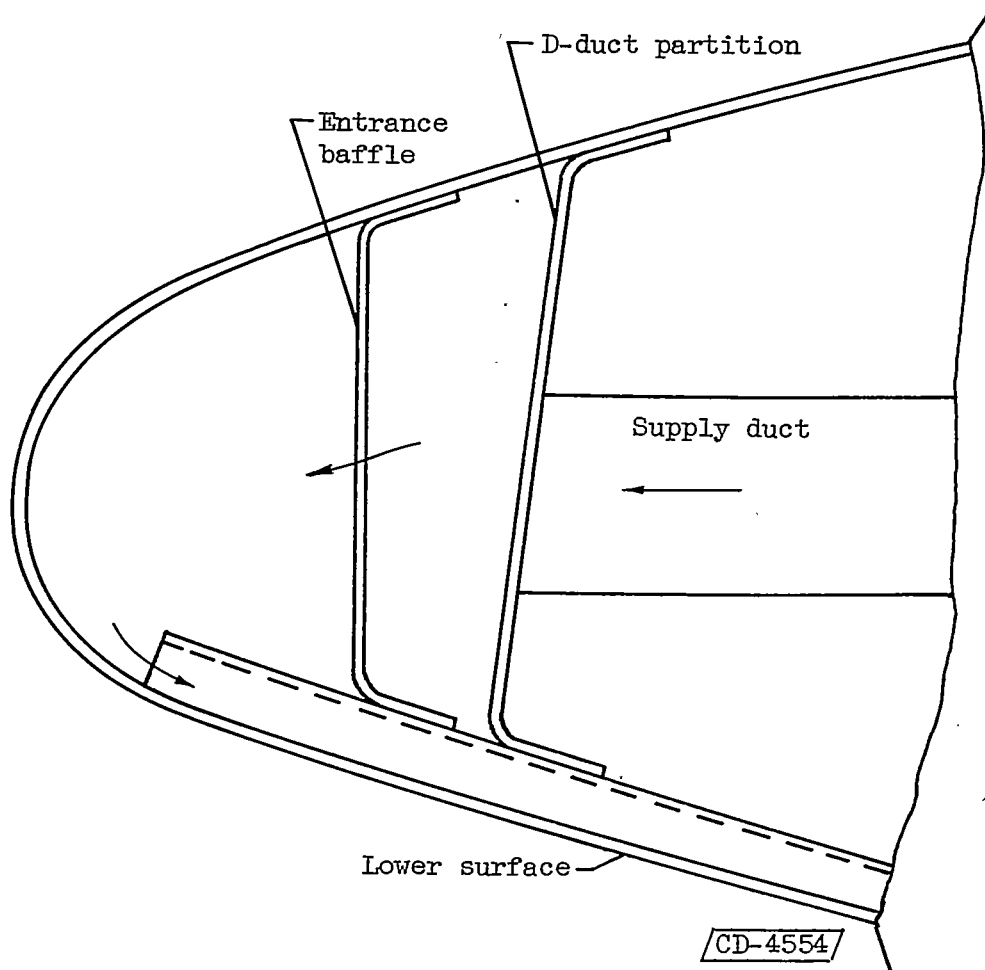
UU-3



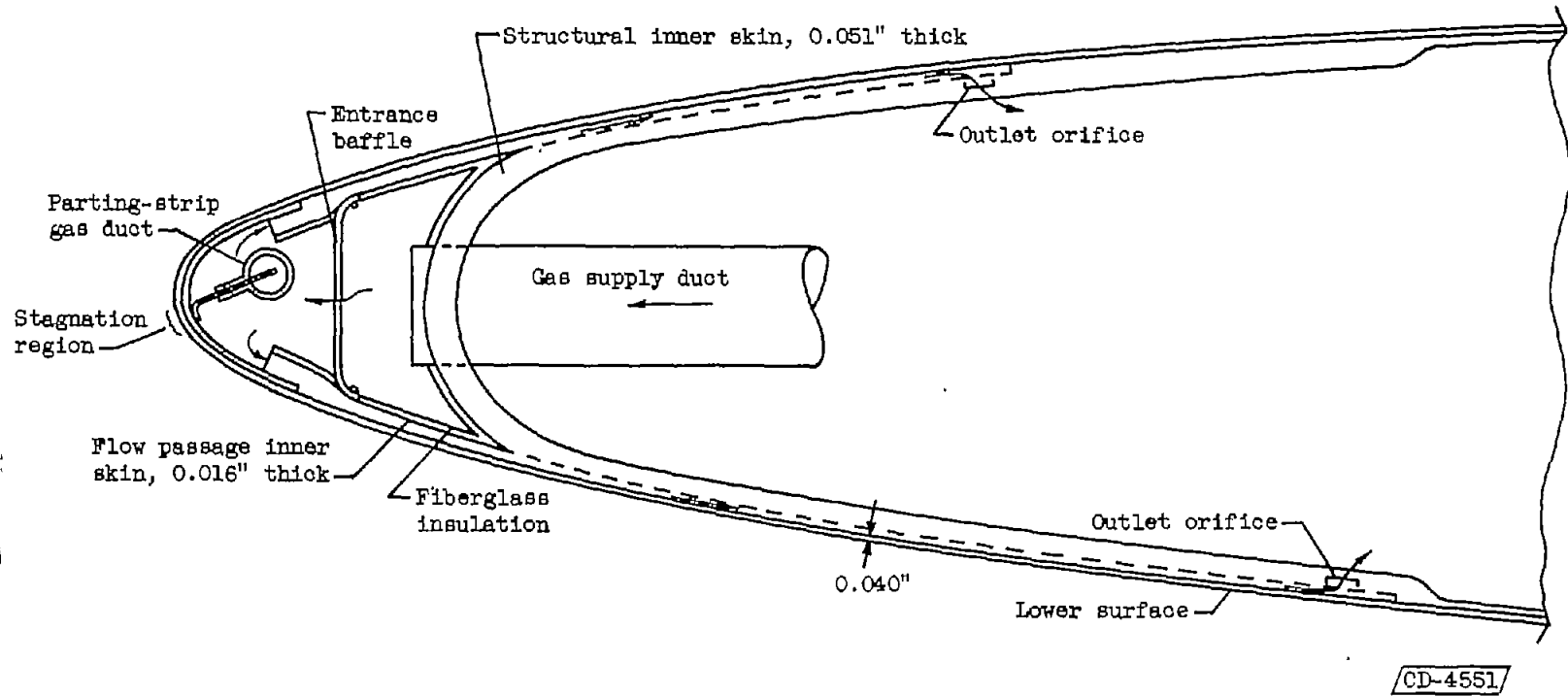
(a) Typical cross section (original version).

Figure 4. - Fixed airfoil behind slat.



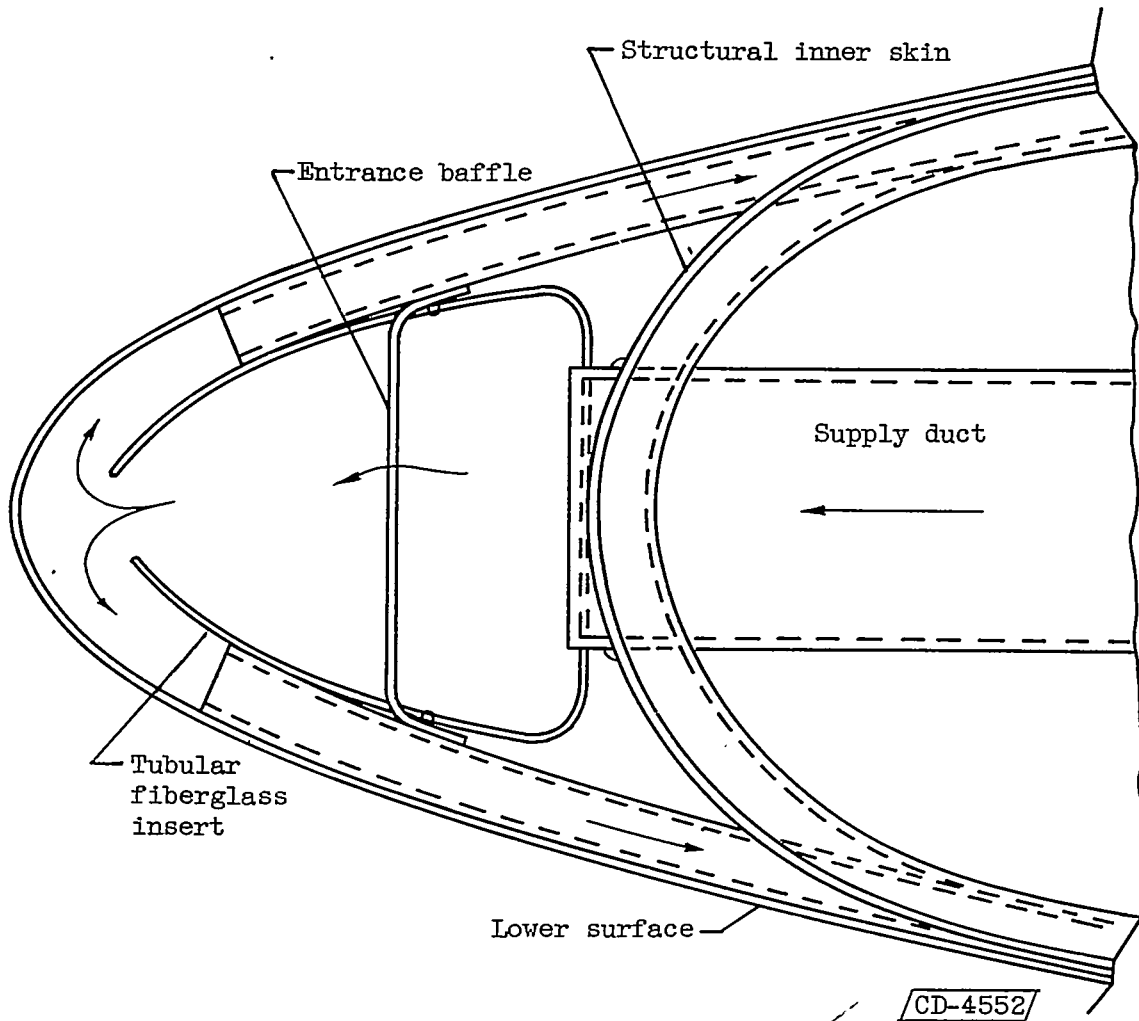


(b) Typical cross section (modified version).  
Figure 4. - Concluded. Fixed airfoil behind slat.



(a) Typical cross section (original version).

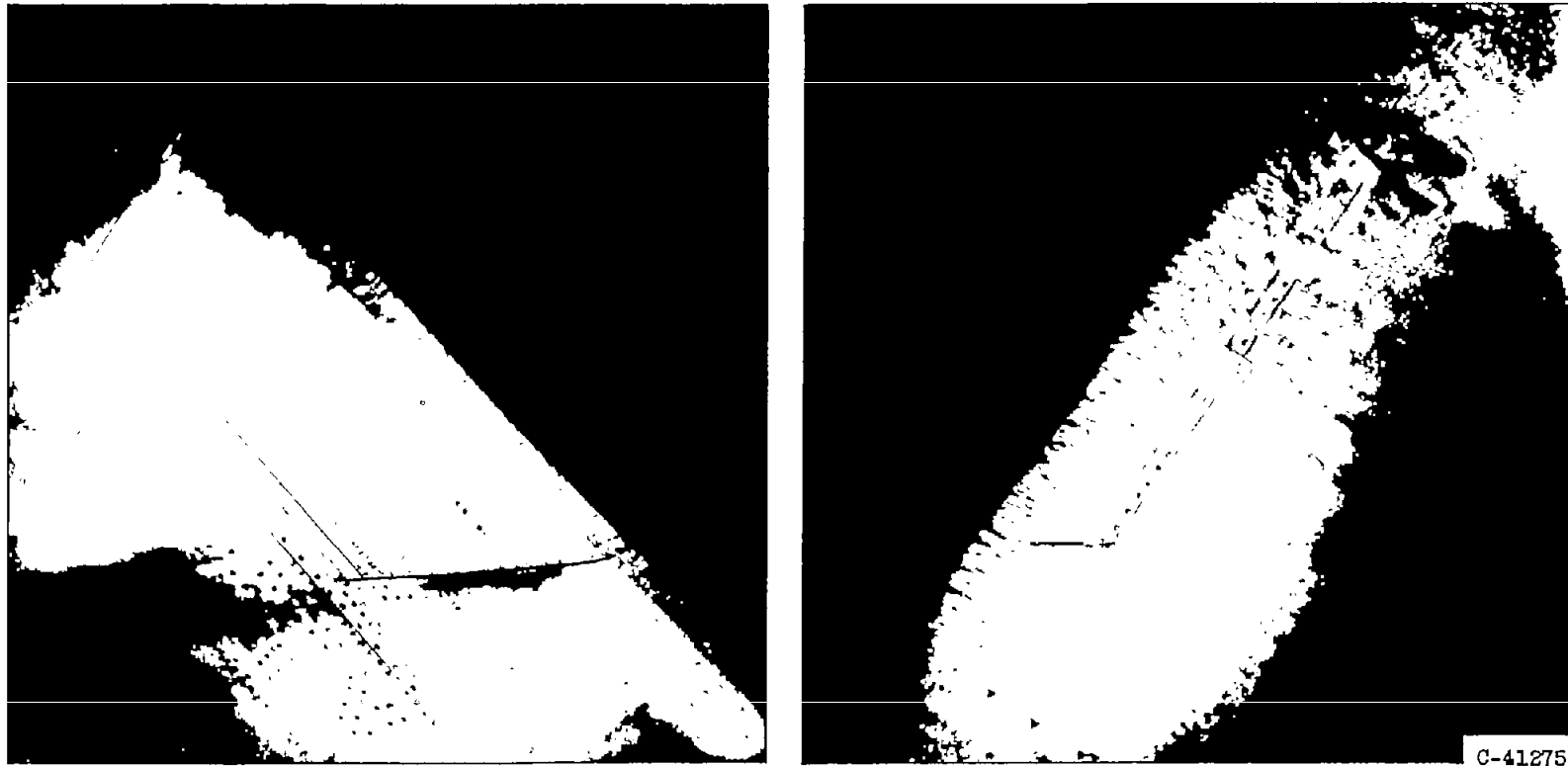
Figure 5. - Standard airfoil.



3081

(b) Typical cross section (modified version).

Figure 5. - Concluded. Standard airfoil.



Upper surface. Icing time,  $5\frac{1}{2}$  minutes.

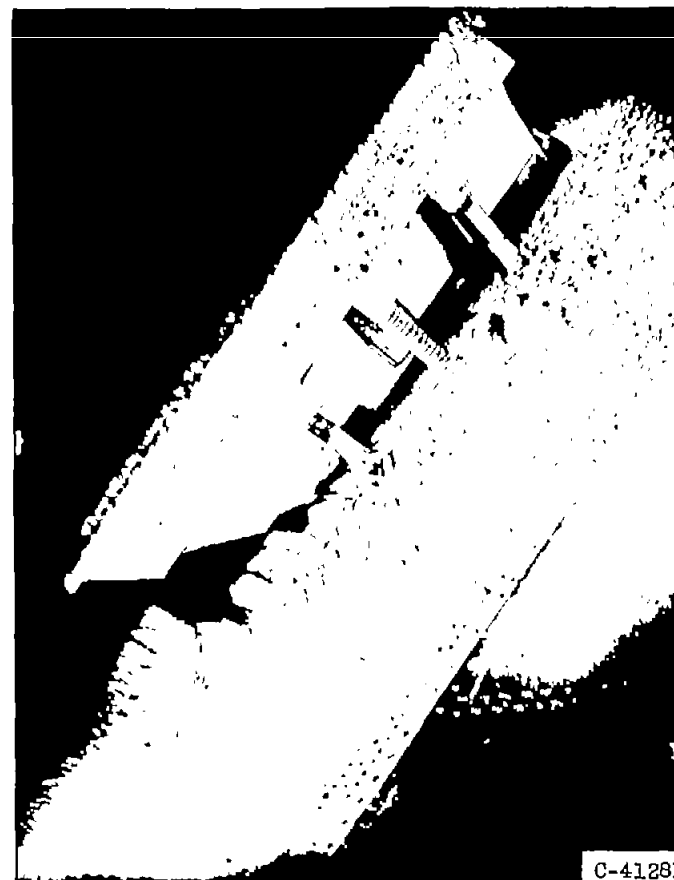
Lower surface. Icing time,  $10\frac{1}{2}$  minutes.

(a) Slat retracted. Airspeed, 260 mph; angle of attack,  $8^\circ$ ; liquid-water content, 0.8 gram per cubic meter.

Figure 6. - Glaze-ice deposits on unheated model. Datum air temperature,  $25^\circ$  F.



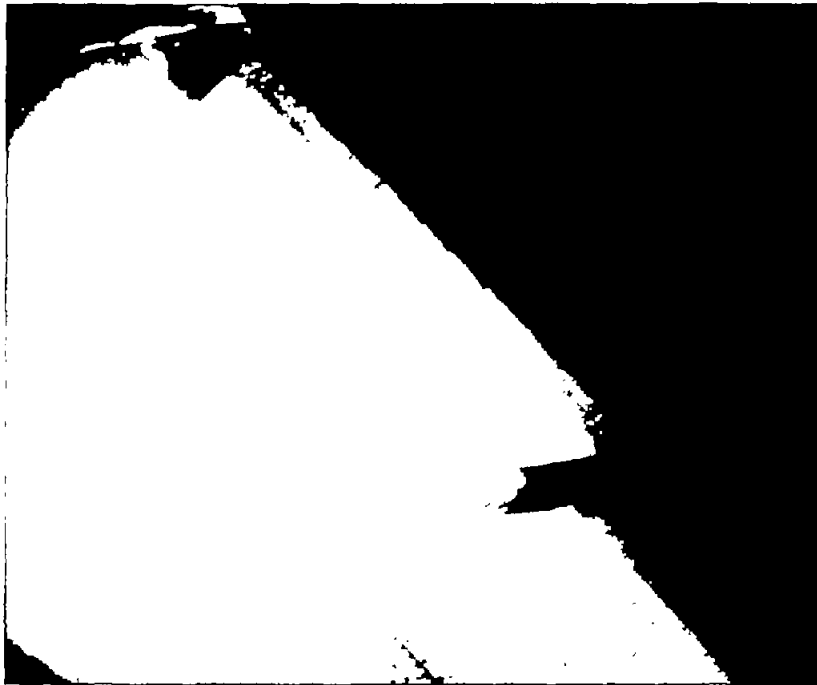
Upper surface. Icing time,  $10\frac{1}{2}$  minutes.



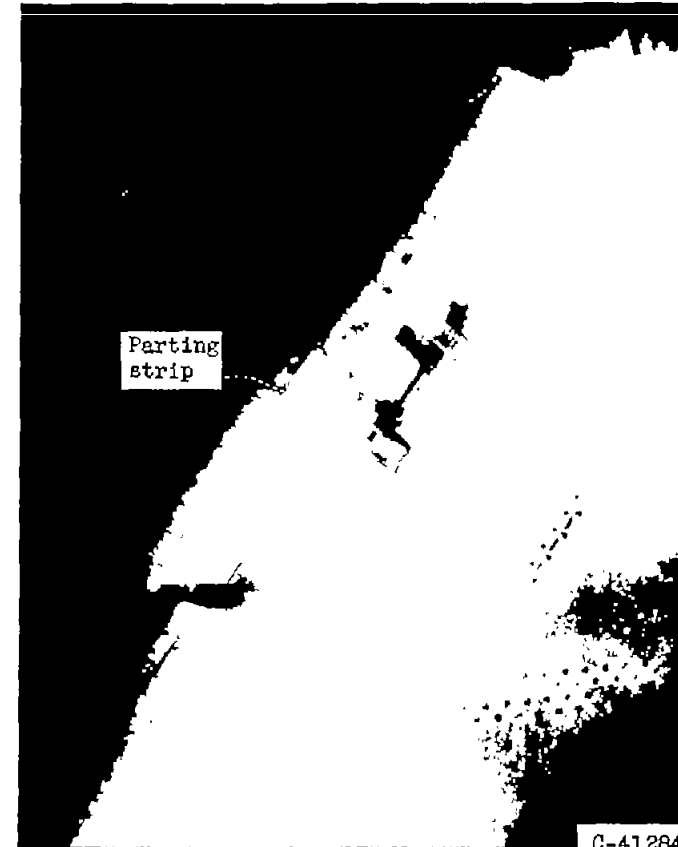
Lower surface. Icing time, 10 minutes.

(b) Slat fully extended. Airspeed, 260 mph; angle of attack,  $8^\circ$ ; liquid-water content, 0.9 gram per cubic meter.

Figure 6. - Continued. Glaze-ice deposits on unheated model. Datum air temperature,  $25^\circ$  F.



Upper surface. Icing time,  $10\frac{1}{2}$  minutes.



Lower surface. Icing time, 10 minutes.

(c) Parting strips heated. Airspeed, 175 mph; angle of attack,  $6^\circ$ ; liquid-water content, 1.1 grams per cubic meter.

Figure 8. - Concluded. Glaze-ice deposits on unheated model. Datum air temperature,  $25^\circ$  F.



(a) Original model. Datum air temperature,  $0^{\circ}$  F; liquid-water content, 0.6 gram per cubic meter.

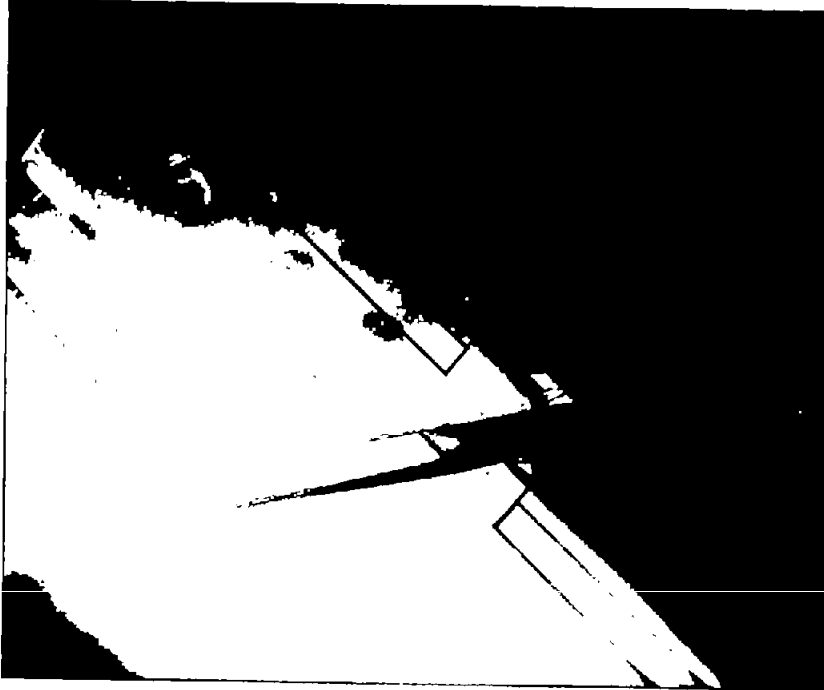
Figure 7. - Insufficiently heated areas of model. Airspeed, 175 mph.



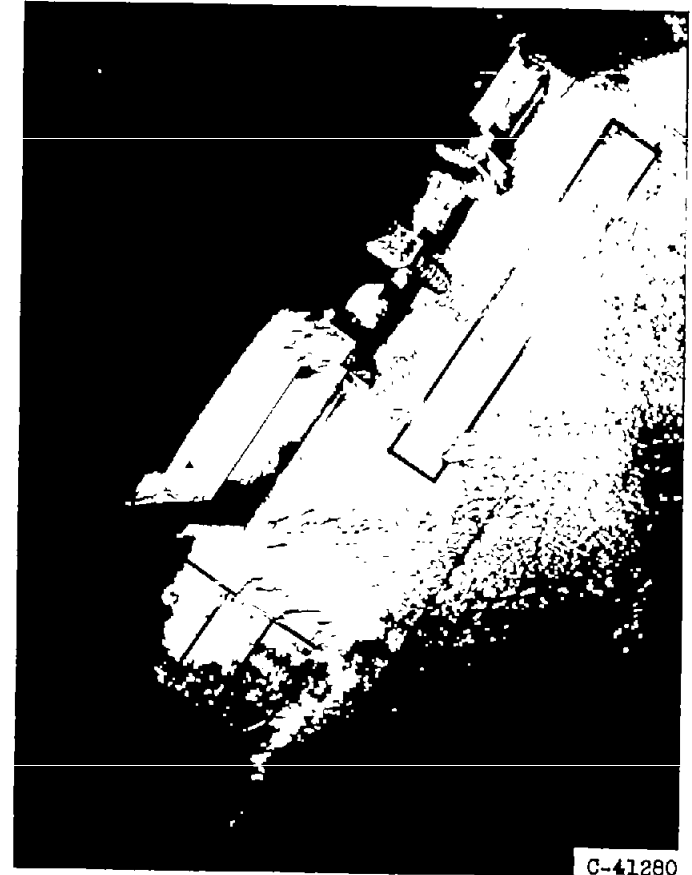
Upper surface. Angle of attack,  $12^{\circ}$ ; icing time, 1 hour 2 minutes.

(a) Concluded. Original model. Datum air temperature,  $0^{\circ}$  F; liquid-water content, 0.6 gram per cubic meter.

Figure 7. - Continued. Insufficiently heated areas of model. Airspeed, 175 mph.



Upper surface. Icing time, 1 hour 1 minute.



Lower surface. Icing time, 57 minutes.

(b) Modified model. Datum air temperature,  $10^{\circ}$  F; liquid-water content, 0.5 gram per cubic meter; angle of attack,  $8^{\circ}$ . (Heating conditions, p. 10.)

Figure 7. - Concluded. Insufficiently heated areas of model. Airspeed, 175 mph.

CONFIDENTIAL

NACA RM E56B23

3081

CC-b DECK



Lower surface, before ice removal. Icing time, 26 minutes.



Lower surface, after ice removal. Icing time,  $26\frac{1}{2}$  minutes.



Upper surface, before ice removal. Icing time, 39 minutes.



Upper surface, after ice removal. Icing time,  $39\frac{1}{2}$  minutes.

(a) Original model, glaze icing. Airspeed, 260 mph; datum air temperature,  $25^{\circ}$  F; angle of attack,  $4^{\circ}$ ; liquid-water content, 0.8 gram per cubic meter.

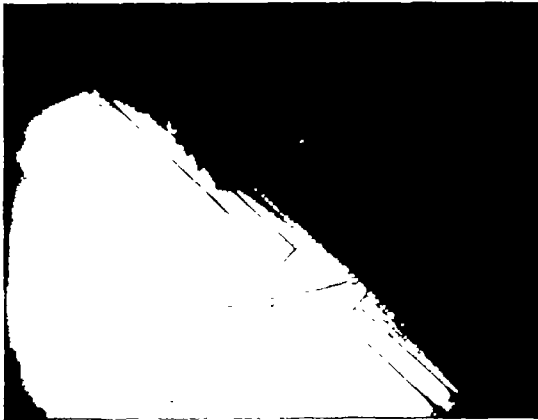
Figure 8. - Typical ice formations during marginal cyclic de-icing. (Heating conditions, p. 10.)



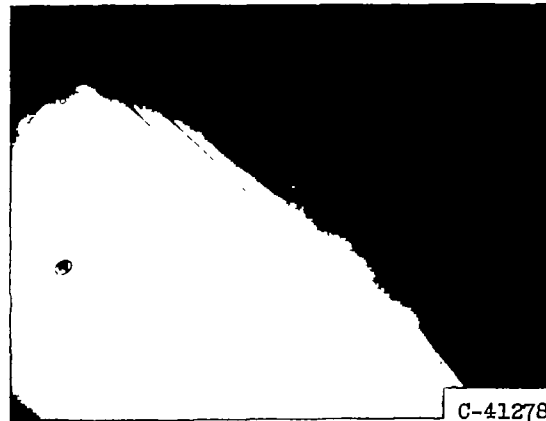
Lower surface, before ice removal.  
Icing time, 40 minutes.



Lower surface, after ice removal.  
Icing time,  $40\frac{1}{2}$  minutes.



Upper surface, before ice removal. Icing time,  
44 minutes.



Upper surface, after ice removal. Icing time,  
 $44\frac{1}{2}$  minutes.

C-41278

(b) Modified model, glaze icing. Airspeed, 260 mph; datum air temperature,  $25^{\circ}$  F; angle of attack,  $4^{\circ}$ ; liquid-water content, 0.7 gram per cubic meter.

Figure 8. - Continued. Typical ice formations during marginal cyclic de-icing. (Heating conditions, p. 10.)

CONFIDENTIAL

TRAC



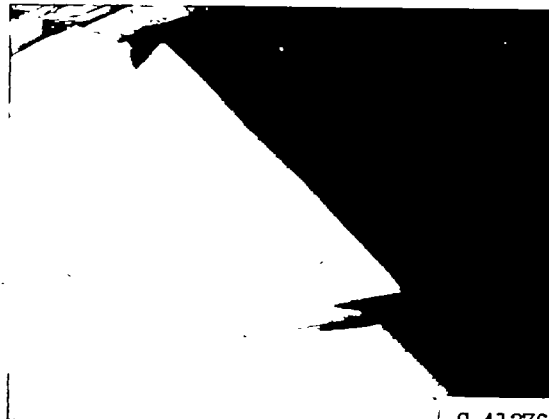
Lower surface, before ice removal. Icing time, 49 minutes.



Lower surface, after ice removal. Icing time, 49½ minutes.



Upper surface, before ice removal. Icing time, 54 minutes.



Upper surface, after ice removal. Icing time, 54½ minutes.

C-41276

(c) Original model, rime icing. Airspeed, 175 mph; datum air temperature, 10° F; angle of attack, 8°; liquid-water content, 0.6 gram per cubic meter.

Figure 8. - Concluded. Typical ice formations during marginal cyclic de-icing. (Heating conditions, p. 10.)

CONFIDENTIAL

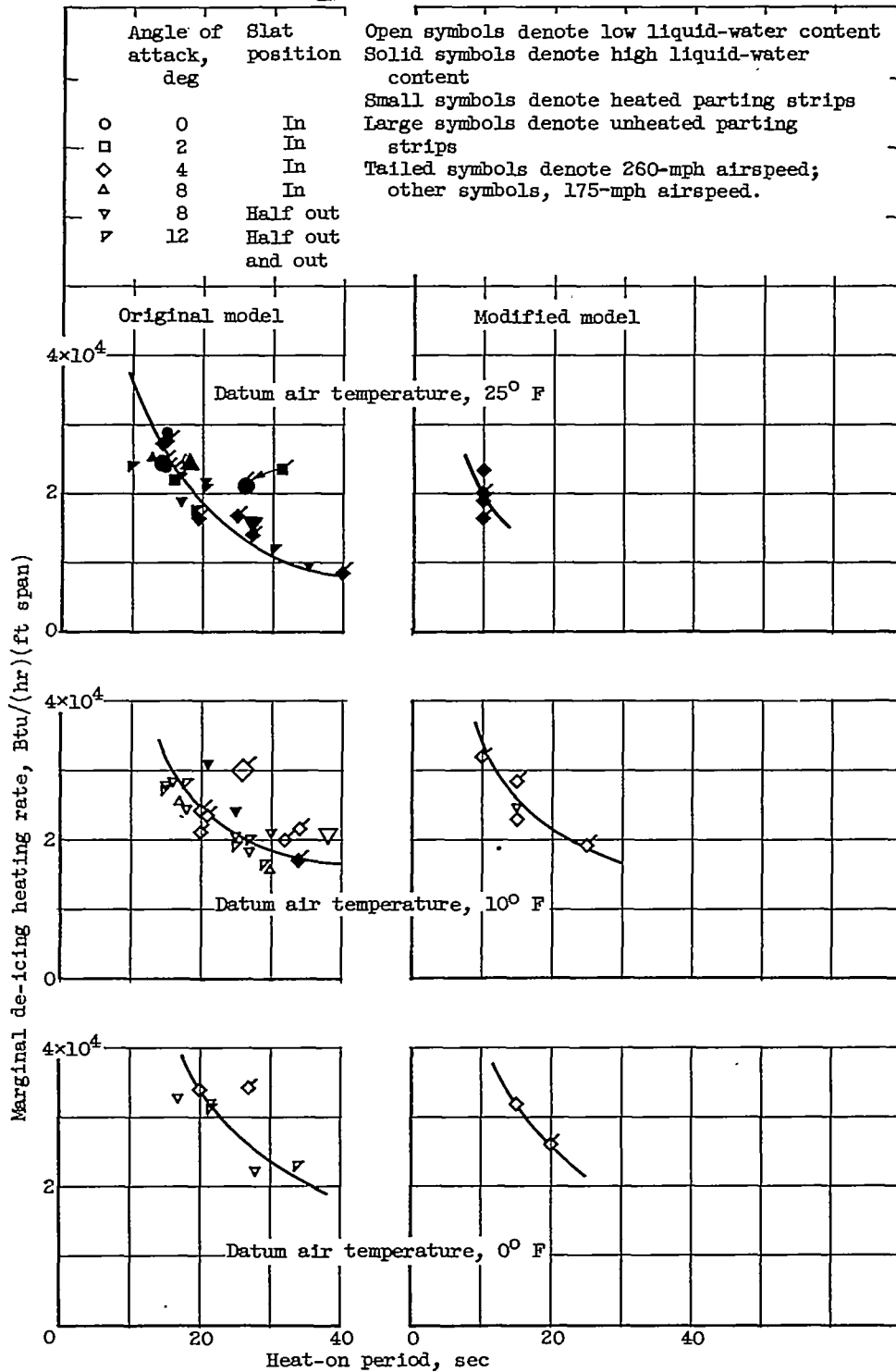


Figure 9. - Marginal de-icing heating rate as a function of heat-on period. Total cycle time, approximately 4 minutes.

3081

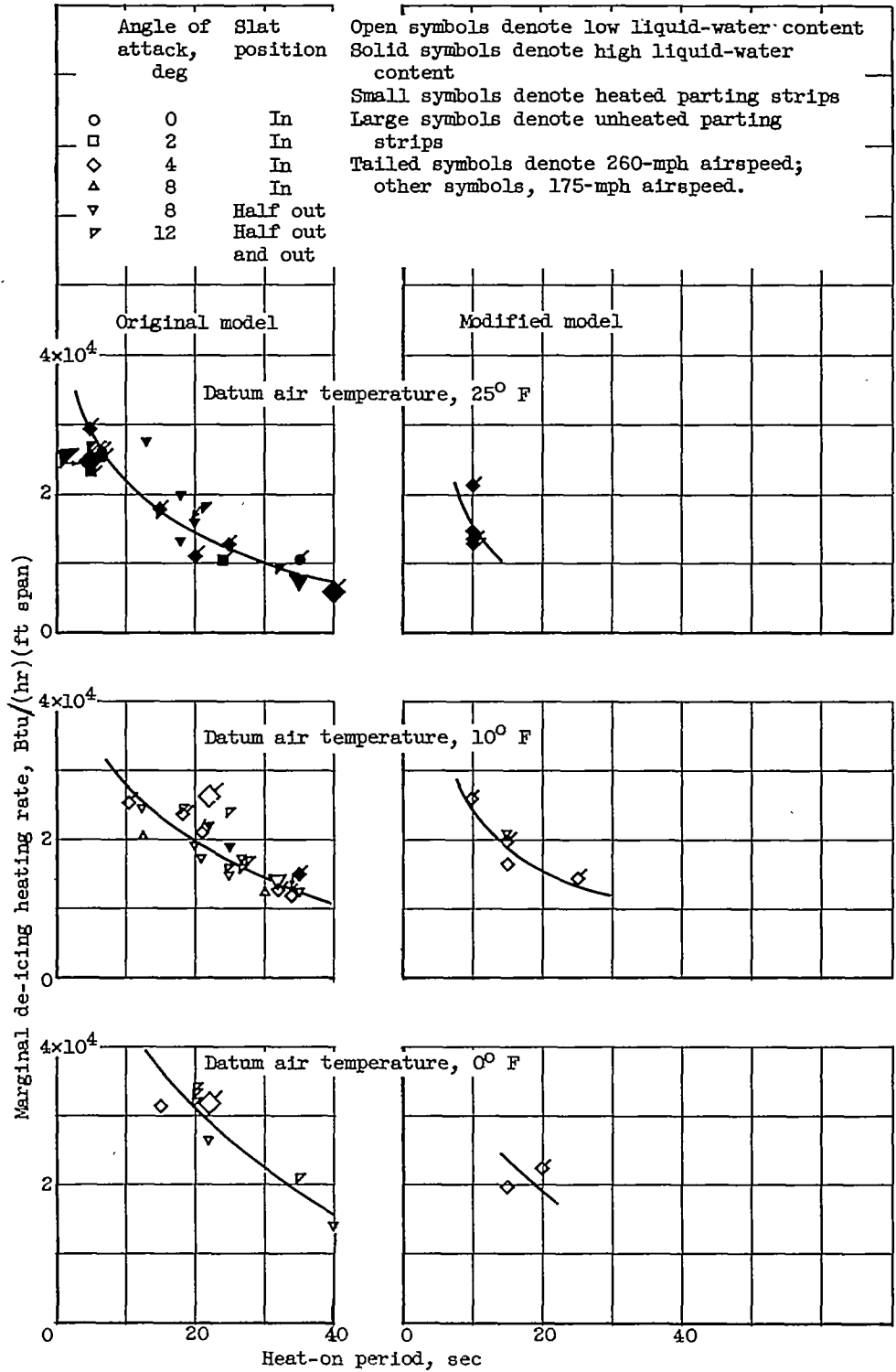
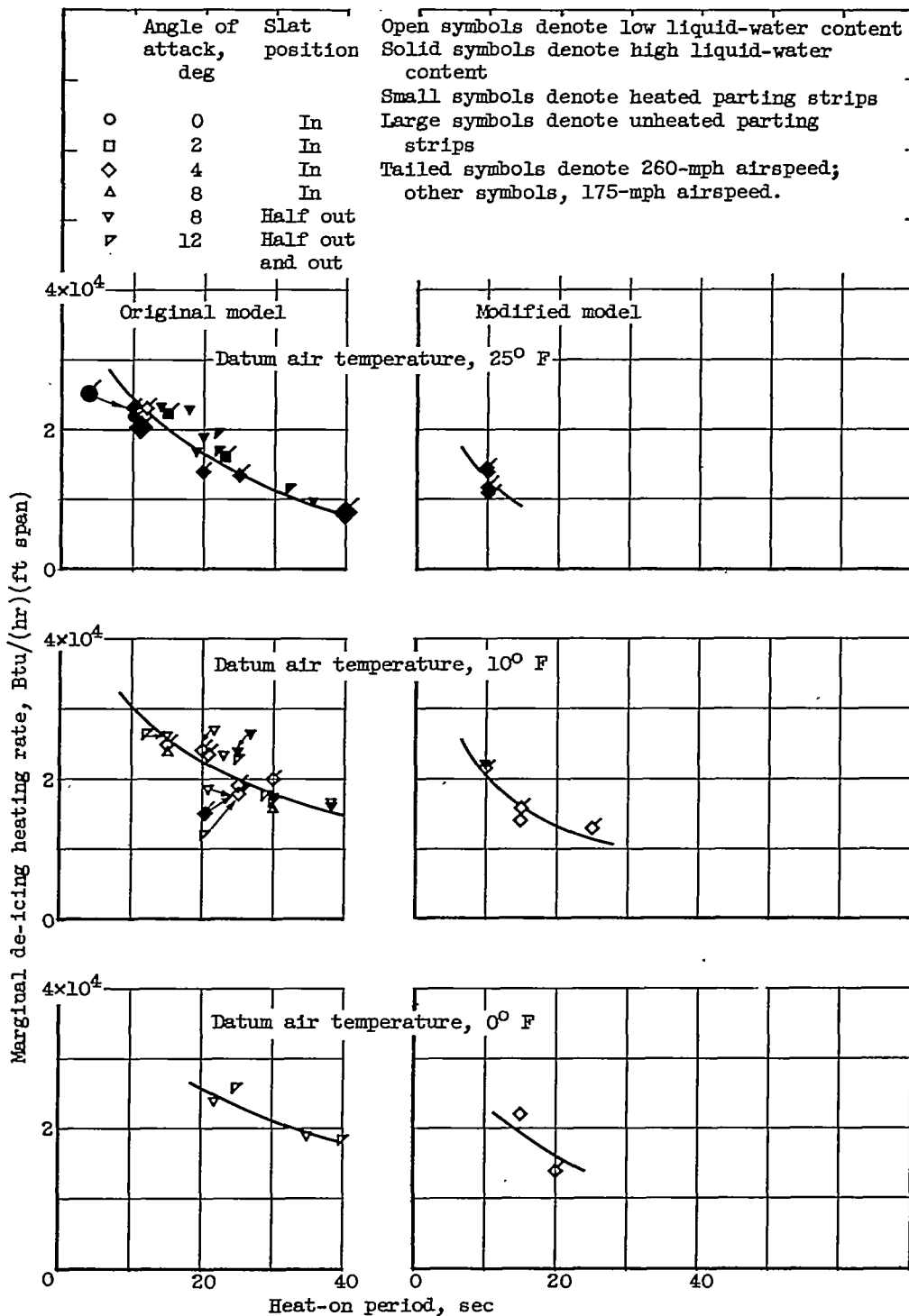


Figure 9. - Continued. Marginal de-icing heating rate as a function of heat-on period. Total cycle time, approximately 4 minutes.



(c) Fixed airfoil.

Figure 9. - Concluded. Marginal de-icing heating rate as a function of heat-on period. Total cycle time, approximately 4 minutes.

3081

CC-7

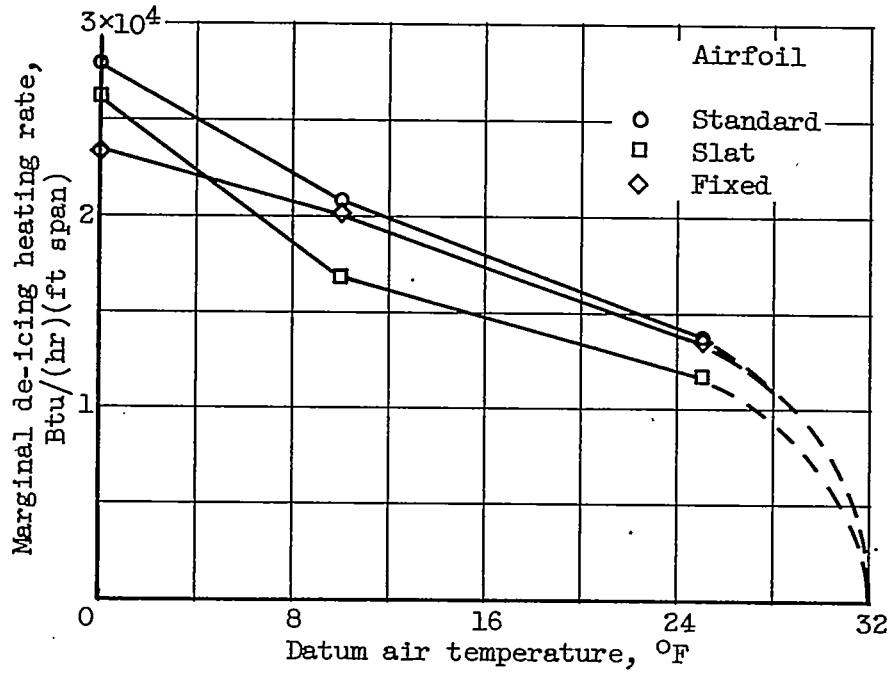
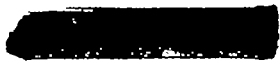


Figure 10. - Effect of datum air temperature on marginal de-icing heating rate (original model). Total cycle time, approximately 4 minutes; heat-on period, 25 seconds.



CONFIDENTIAL

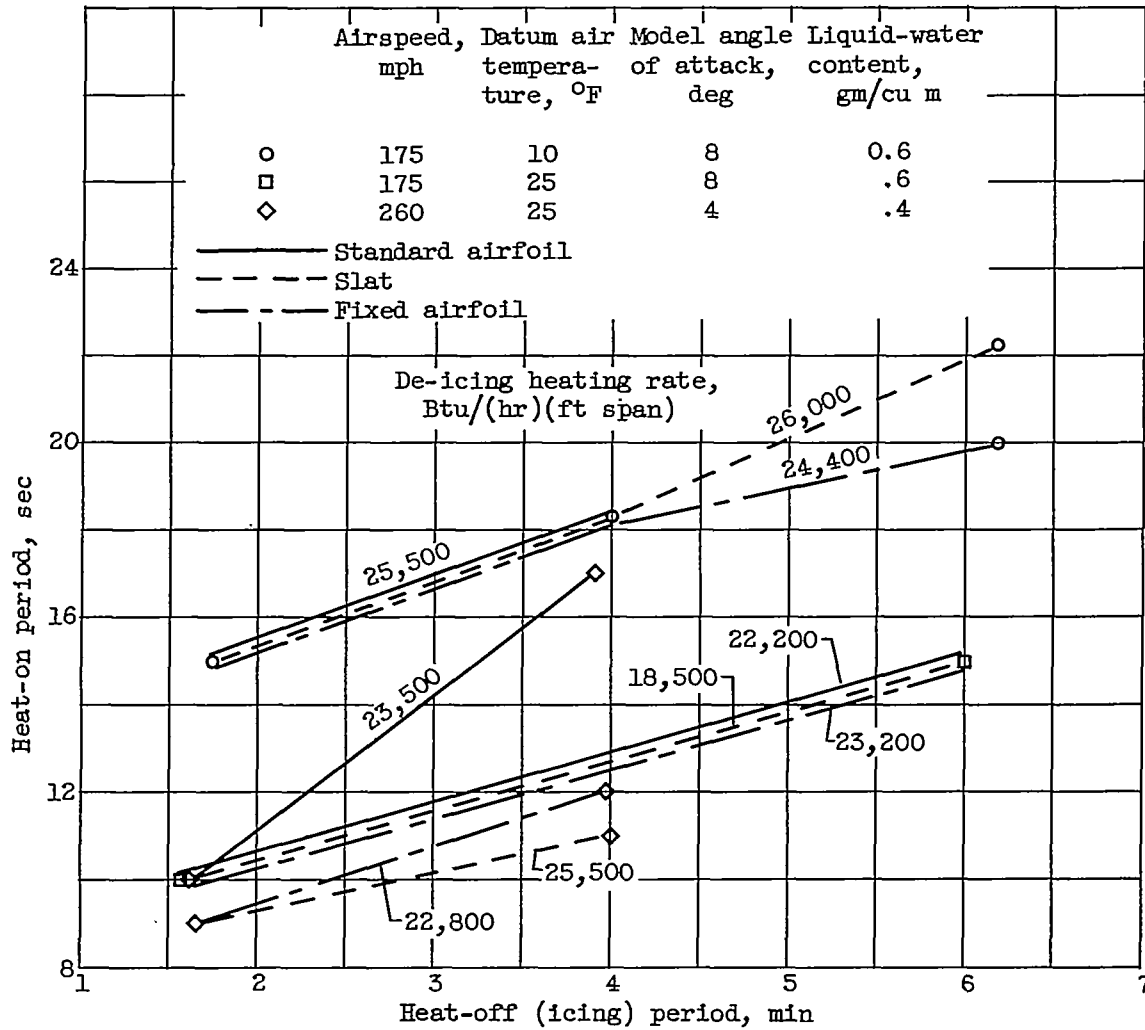
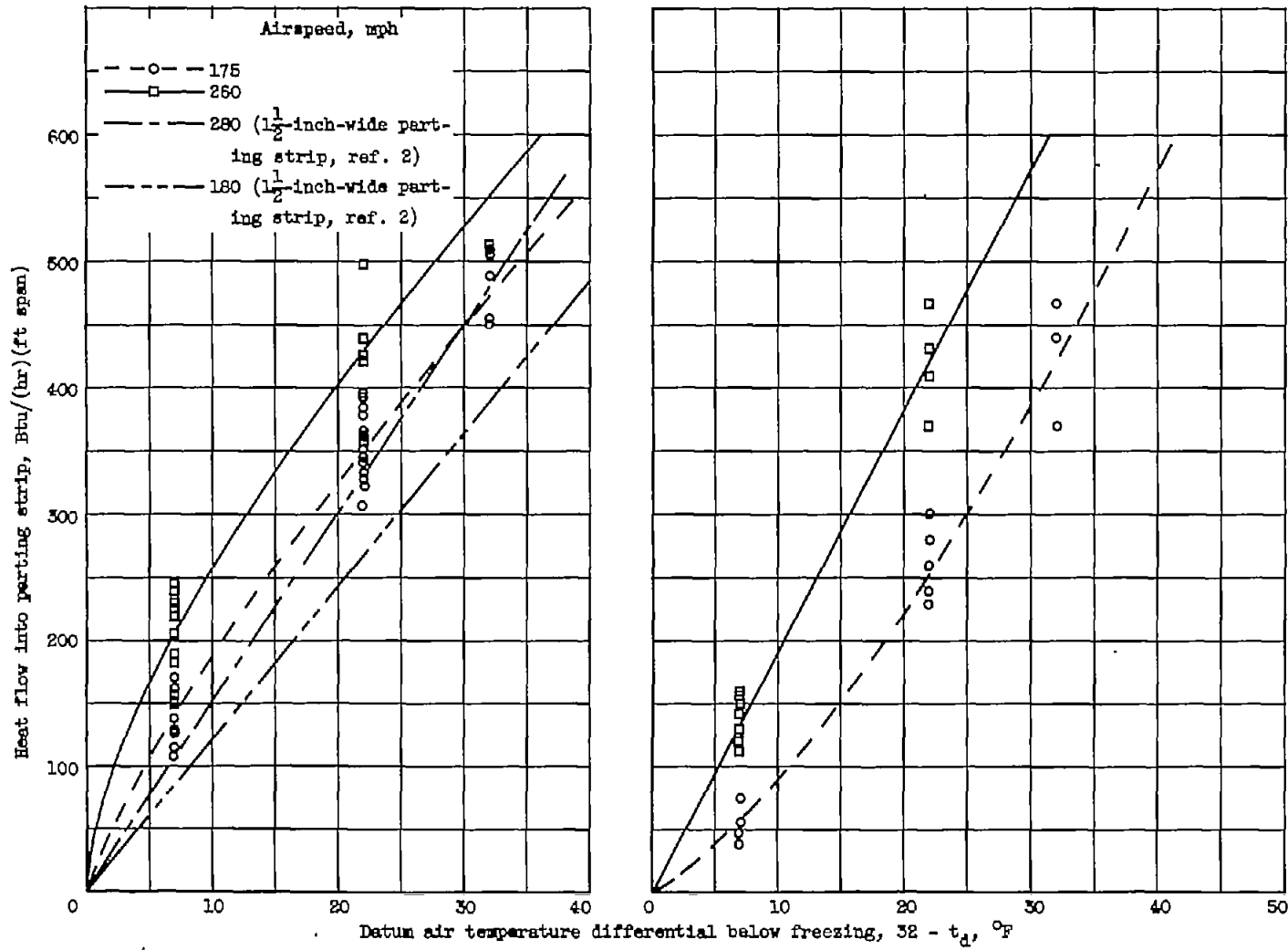


Figure 11. - Effect of heat-off (icing) period on heat-on period for marginal de-icing with heated parting strips.

3081

CONFIDENTIAL



(a) Standard airfoil; gas-heated parting strip.

(b) Slat; electric parting strip.

Figure 12. - Heat flow to parting strips as a function of datum air temperature (original model).

CONFIDENTIAL

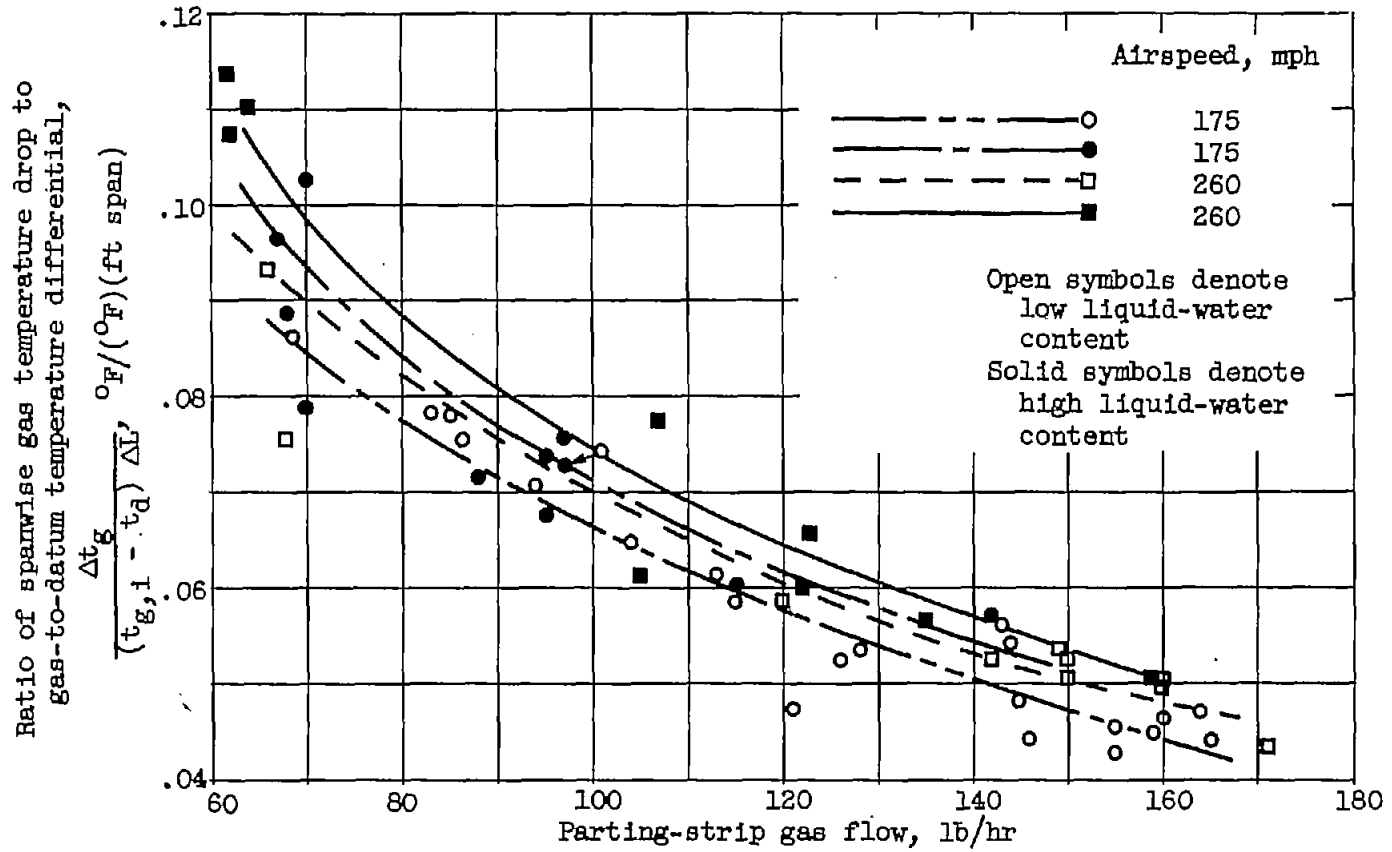
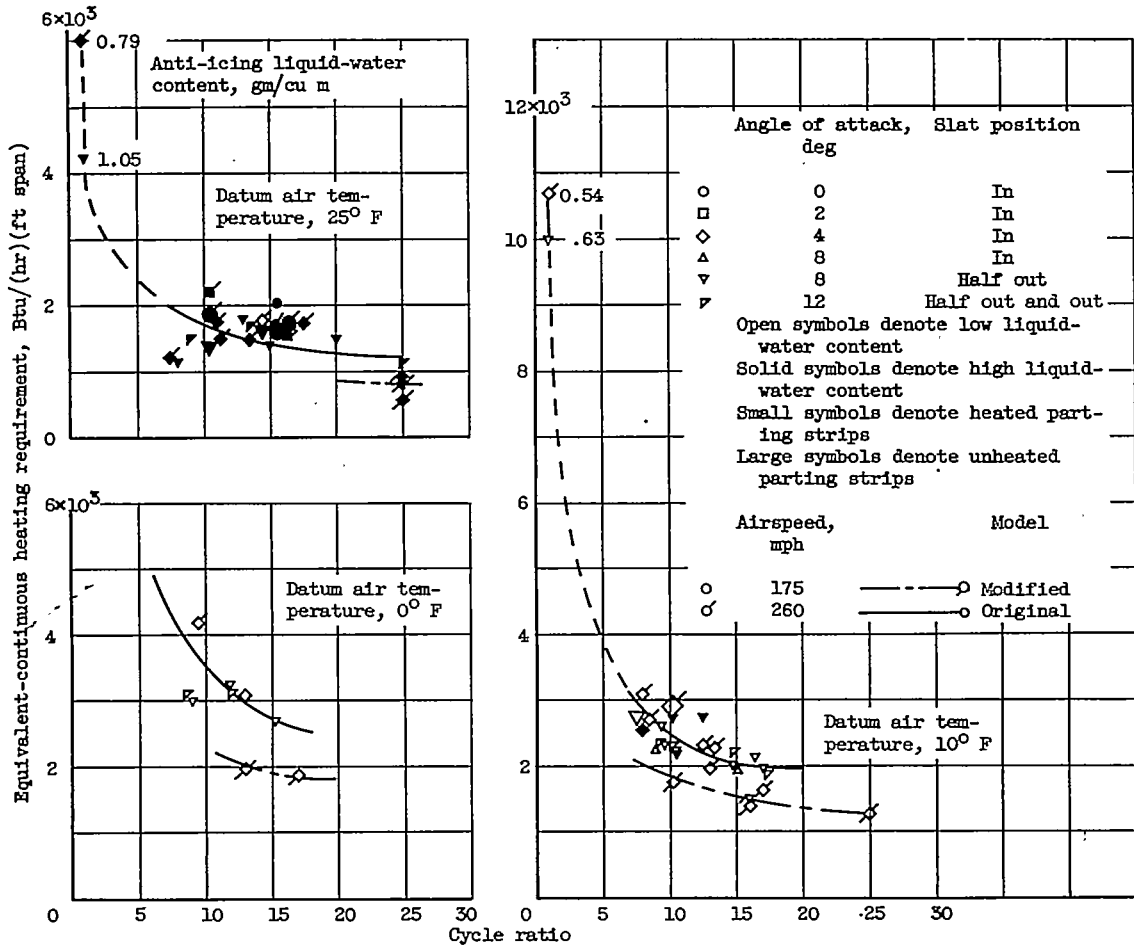


Figure 13. - Spanwise gas temperature drop in standard-airfoil parting-strip duct as function of gas flow and gas-to-datum temperature differential.

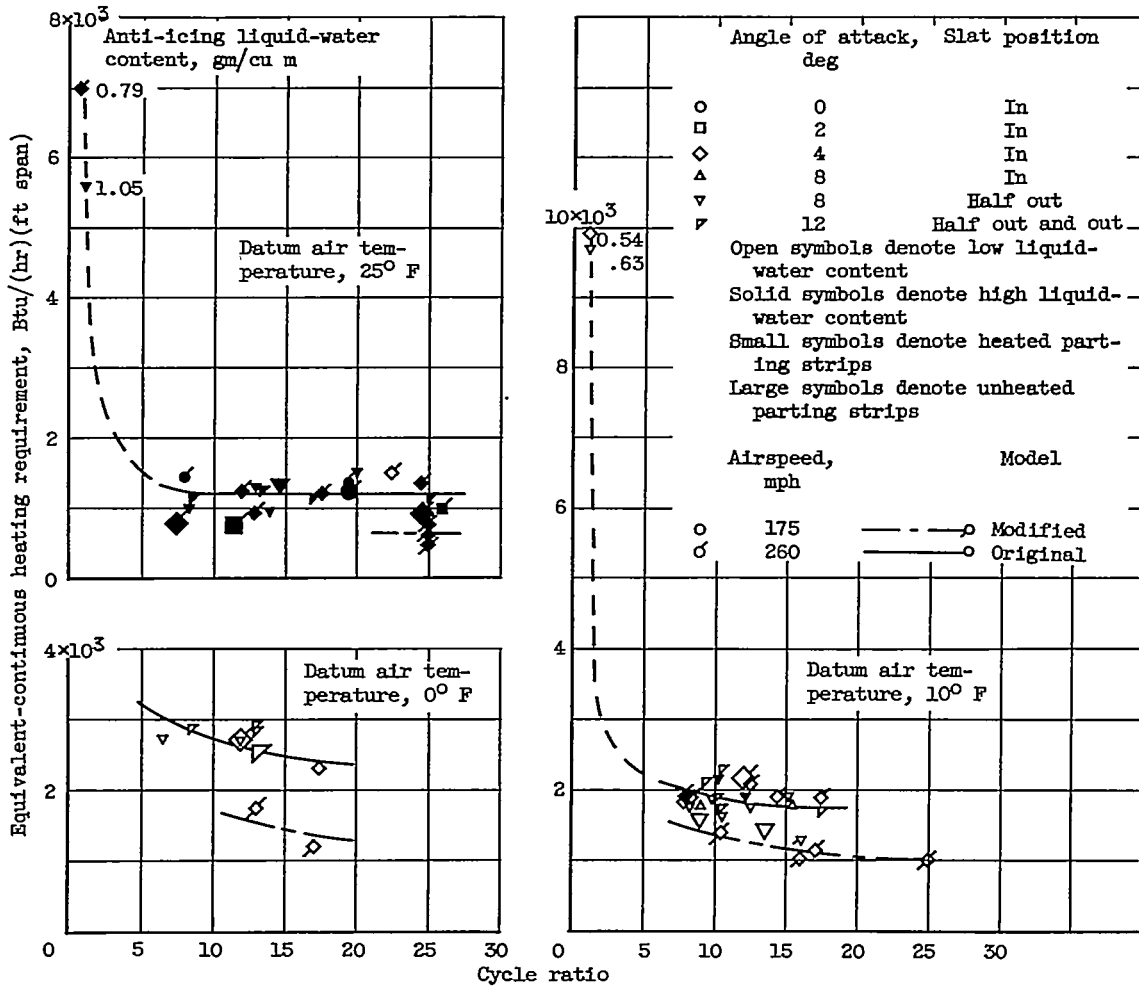
CONFIDENTIAL

5081



(a) Standard airfoil.

Figure 14. - Equivalent-continuous heating requirement as function of cycle ratio. Total cycle time, approximately 4 minutes.

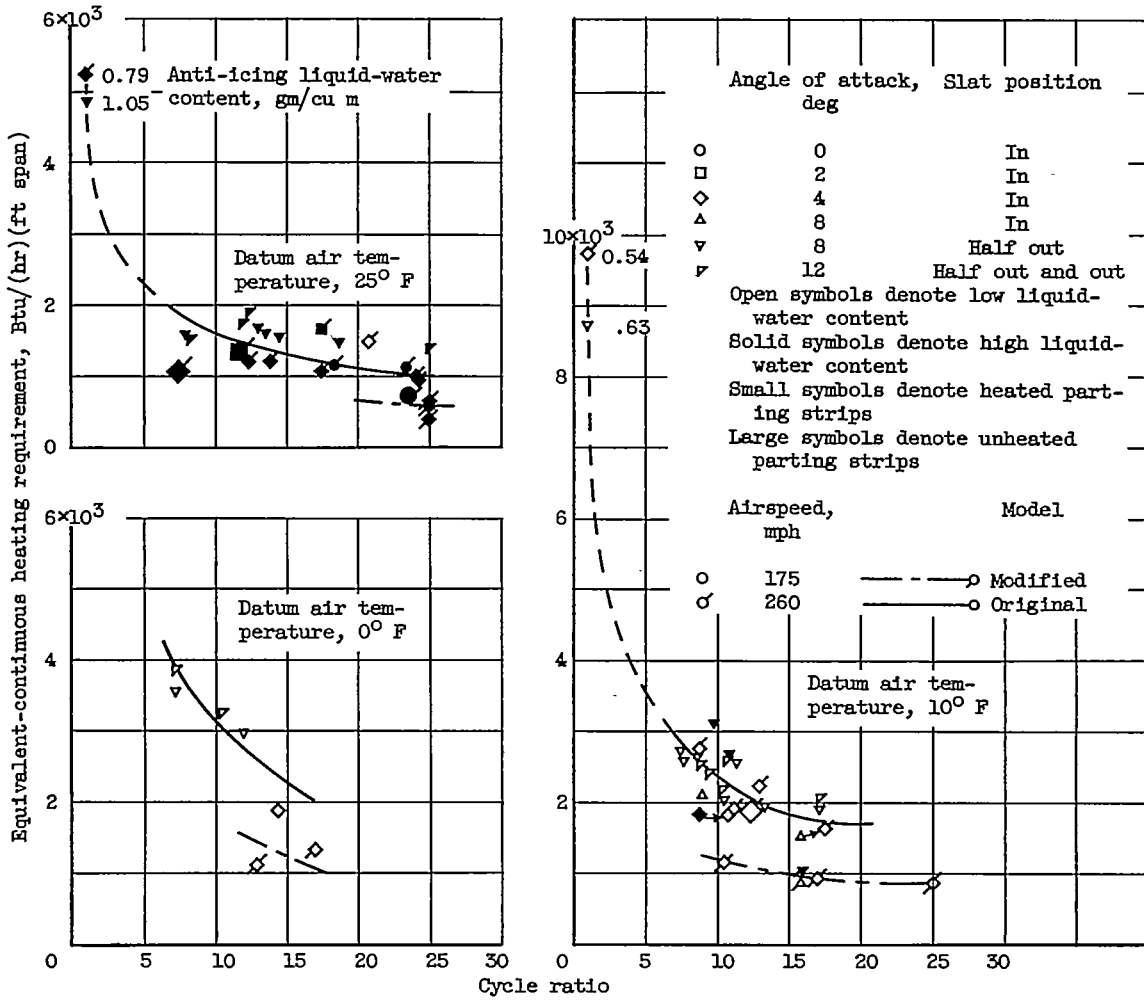


TOP

(b) Slat.

Figure 14. - Continued. Equivalent-continuous heating requirement as function of cycle ratio. Total cycle time, approximately 4 minutes.

3081



(c) Fixed airfoil.

Figure 14. - Concluded. Equivalent-continuous heating requirement as function of cycle ratio. Total cycle time, approximately 4 minutes.

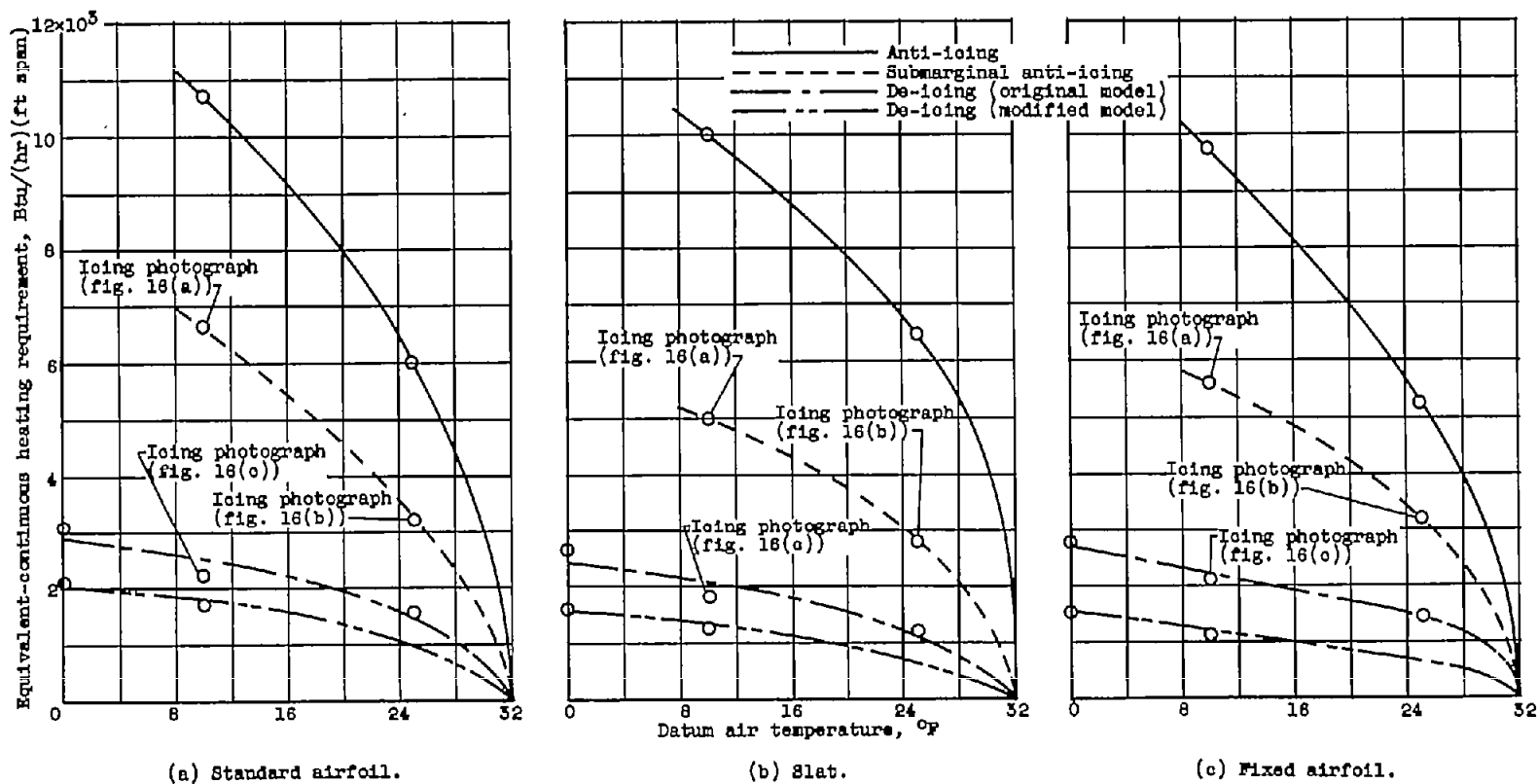


Figure 15. - Comparison of anti-icing and de-icing heat requirements. Airspeed, 280 mph; angle of attack,  $4^{\circ}$ ; slat retracted; de-icing cycle ratio, 12; liquid-water content, 0.5 to 0.8 gram per cubic meter.

CONFIDENTIAL

CONFIDENTIAL



Lower surface



Upper surface

C-41285

(a) Submarginal anti-icing. Datum air temperature,  $10^{\circ}$  F; liquid-water content, 0.5 gram per cubic meter; icing time, 9 minutes.

Figure 16. - Comparison of ice formations resulting from submarginal anti-icing and marginal de-icing. Airspeed, 260 mph; angle of attack,  $4^{\circ}$ ; slat retracted; for heating rates, see figure 15.



Lower surface



Upper surface

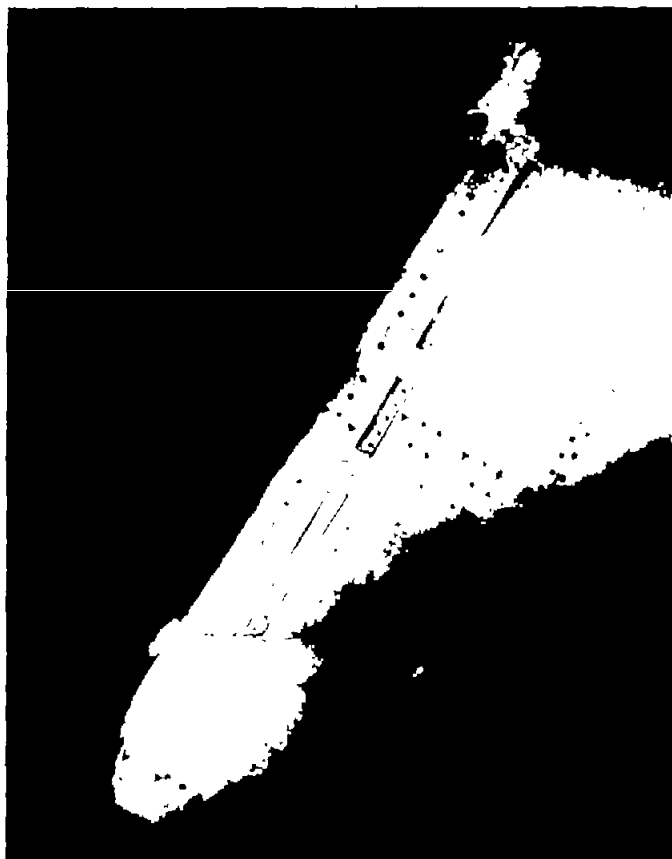
(b) Submarginal anti-icing. Datum air temperature,  $25^{\circ}$  F; liquid-water content, 0.8 gram per cubic meter; icing time, 6 minutes.

Figure 16. - Continued. Comparison of ice formations resulting from submarginal anti-icing and marginal de-icing. Airspeed, 260 mph; angle of attack,  $4^{\circ}$ ; slat retracted; for heating rates, see figure 15.

CONFIDENTIAL

CONFIDENTIAL

NACA RM E56B23



Lower surface, after ice removal.



Upper surface, after ice removal.

(c) Marginal de-icing. Datum air temperature,  $10^{\circ}$  F; liquid-water content, 0.5 gram per cubic meter; icing time, 77 minutes; cycle ratio, 10 to 13.

Figure 16. - Concluded. Comparison of ice formations resulting from submarginal anti-icing and marginal de-icing. Airspeed, 260 mph; angle of attack,  $4^{\circ}$ ; slat retracted; for heating rates, see figure 15.

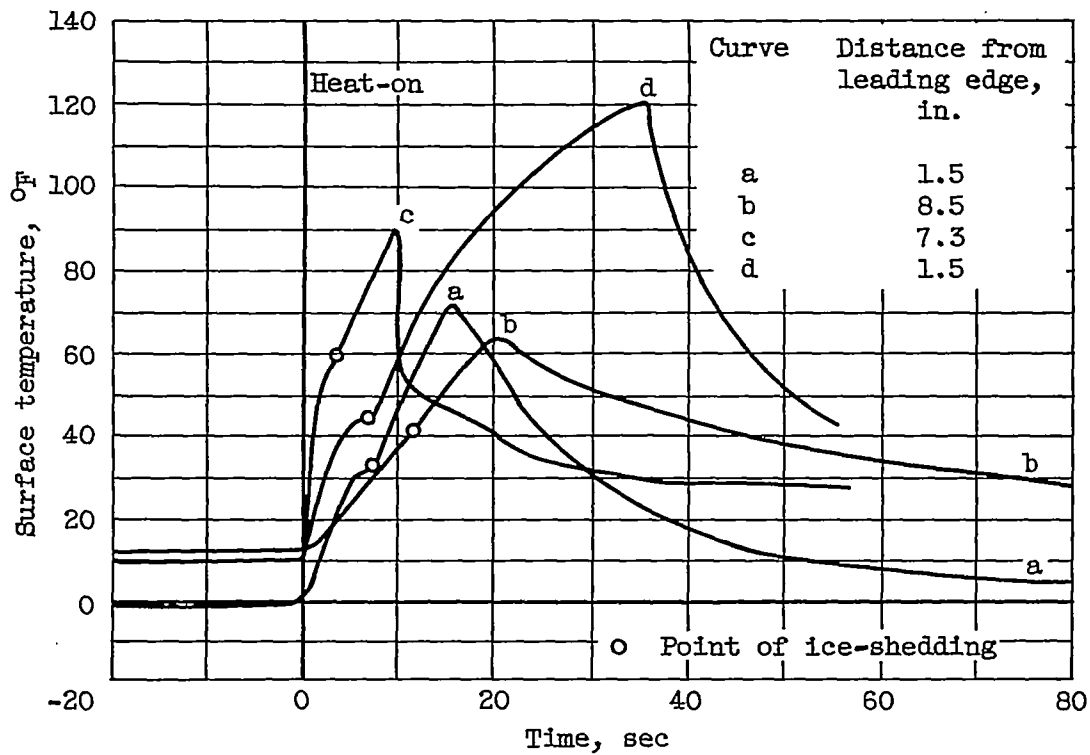


Figure 17. - Representative surface temperature-time curves showing shedding of ice. Conditions listed in table I.

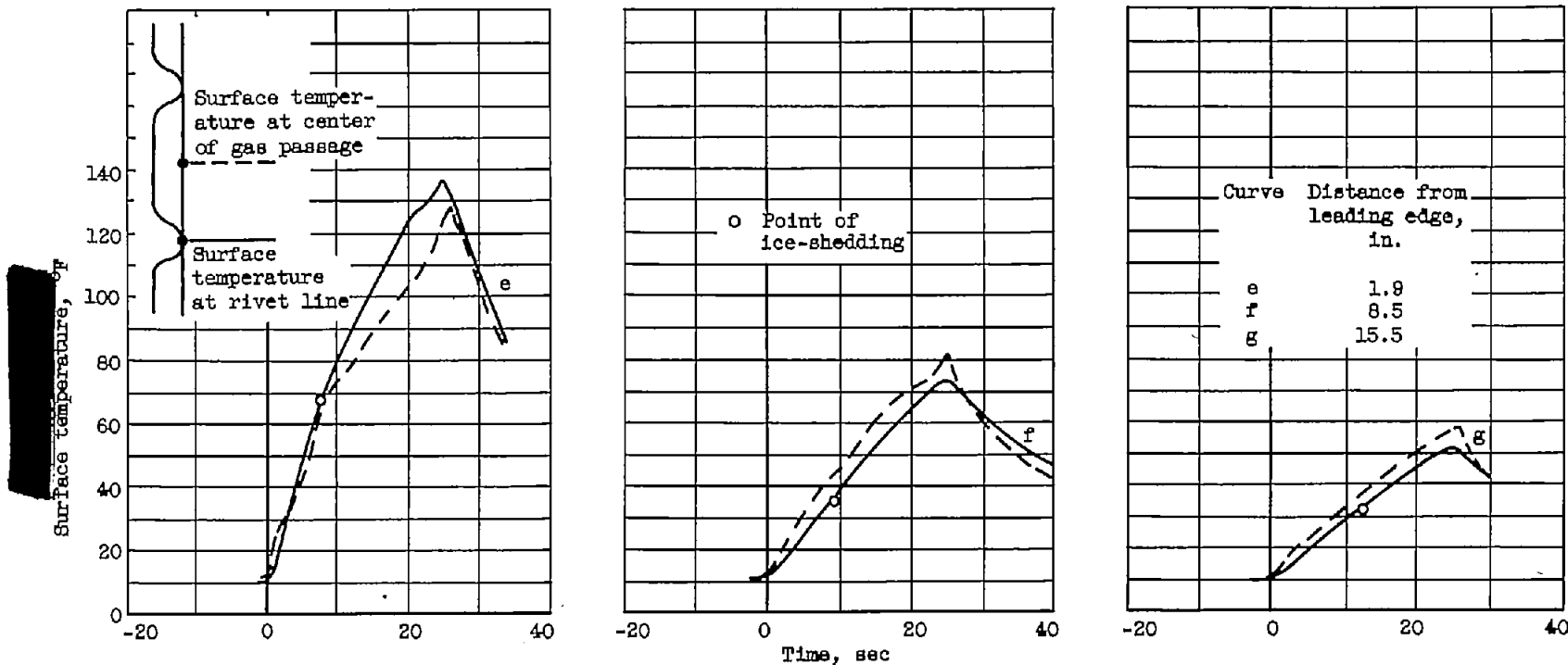
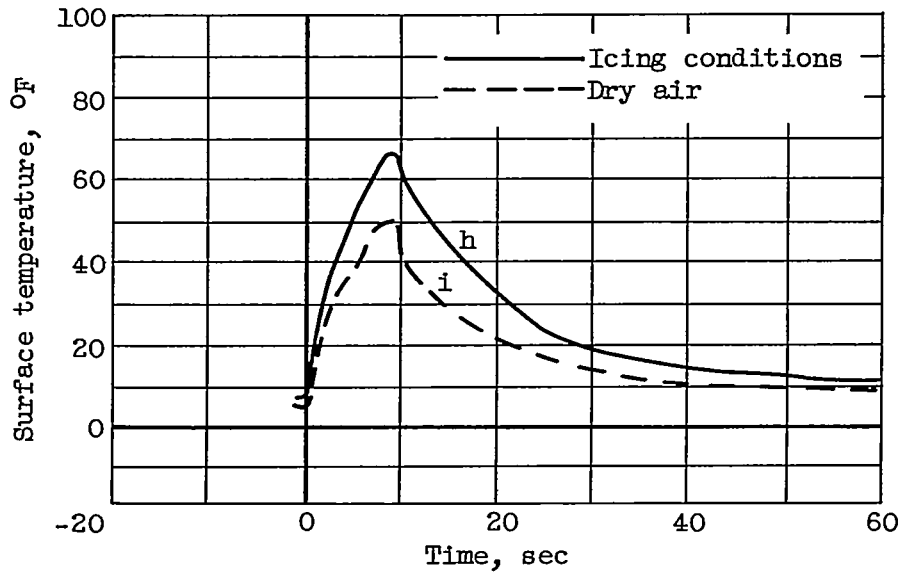


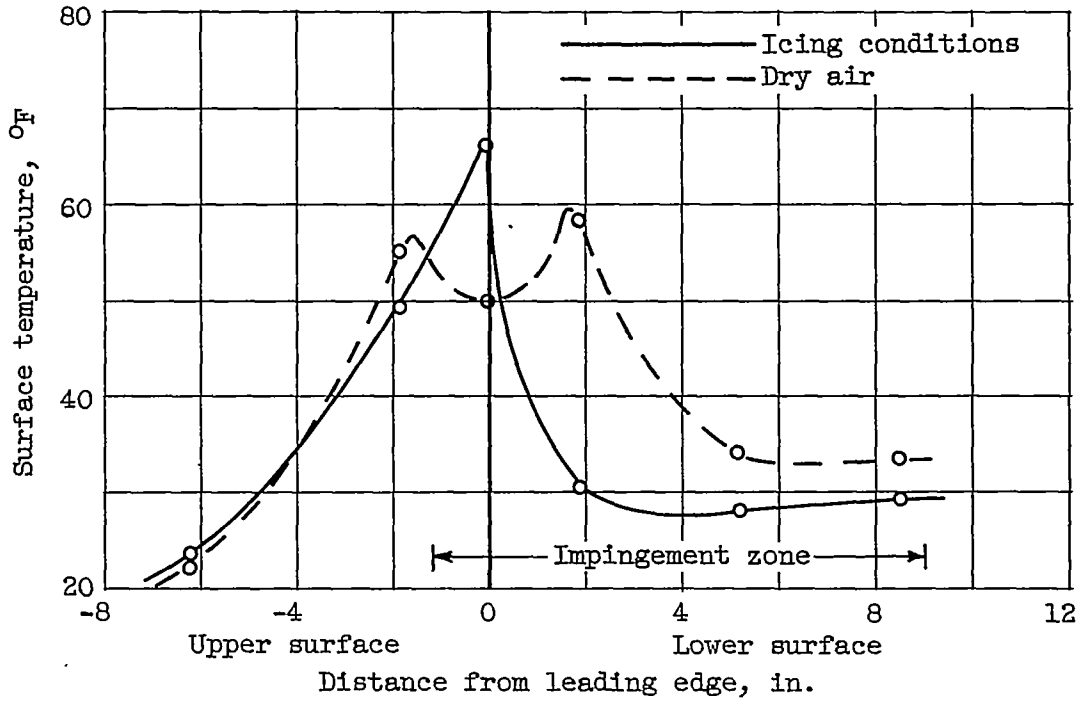
Figure 18. - Concurrent temperature-time curves for six lower-surface thermocouples on original standard airfoil. Conditions listed in table I.



(a) Temperature-time curves for leading-edge thermocouple.

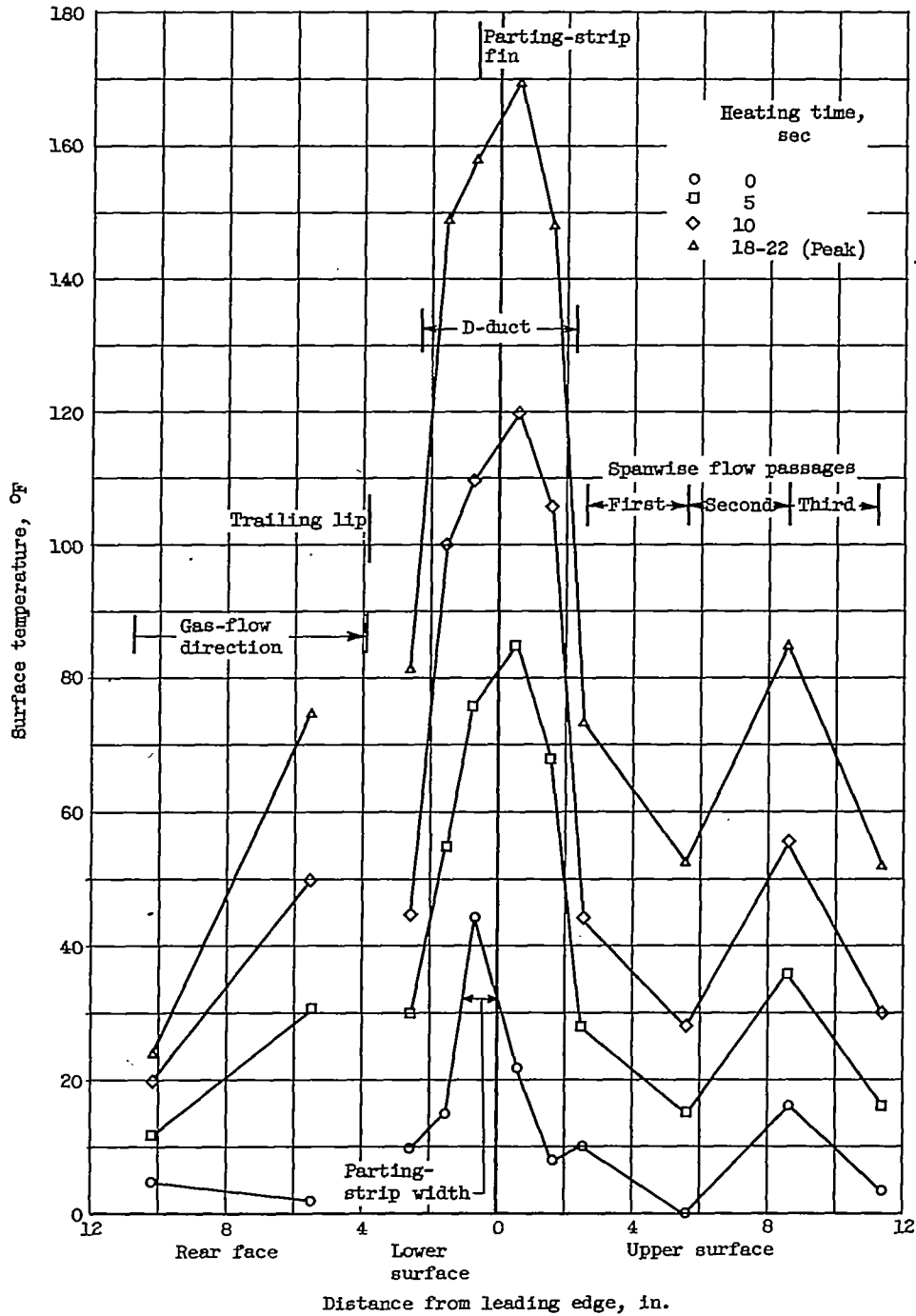
Figure 19. - Comparison of surface temperature curves in dry air and icing conditions. Conditions listed in table I.

3081



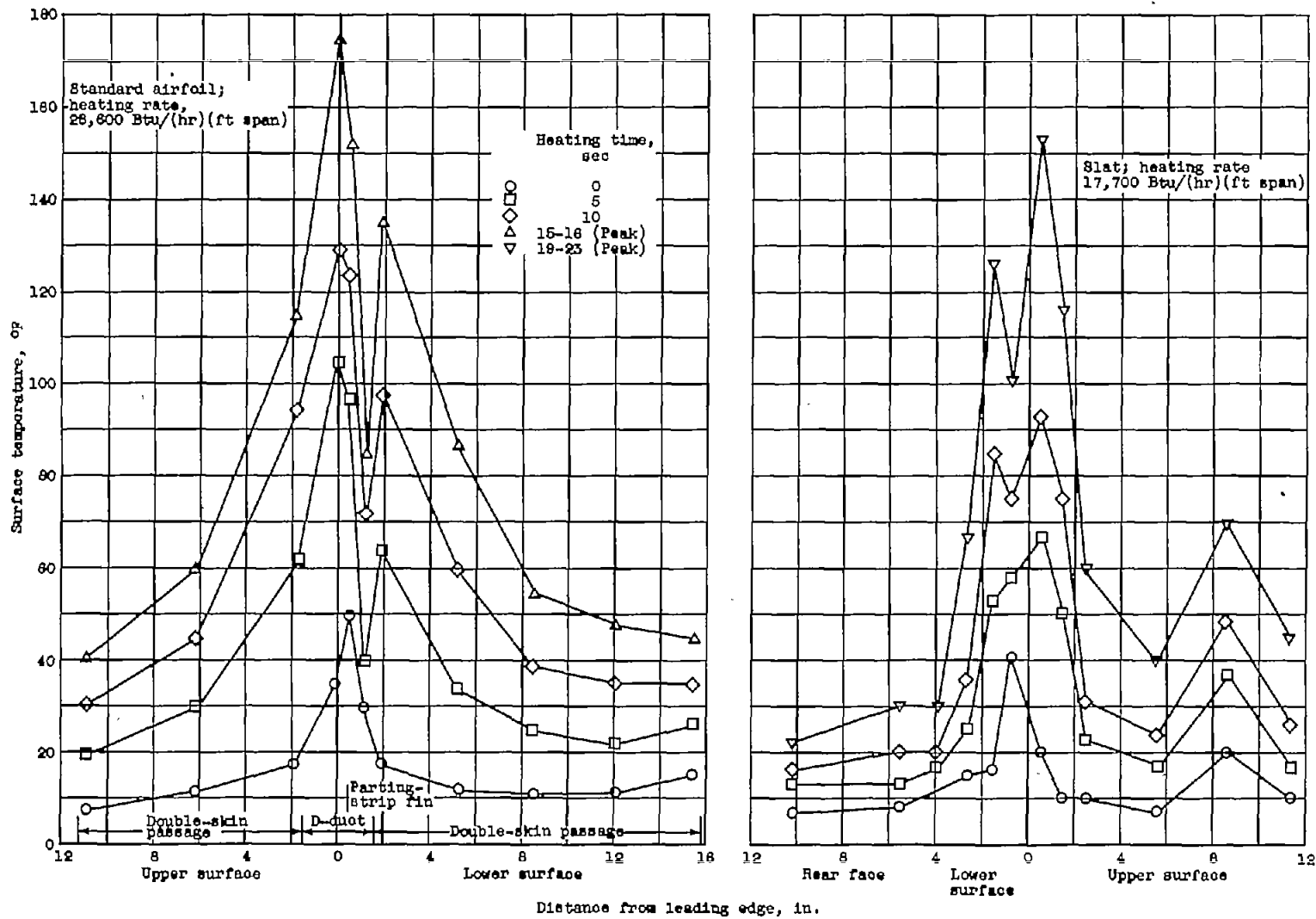
(b) Surface variation of peak temperature.

Figure 19. - Concluded. Comparison of surface temperature curves in dry air and icing conditions. Conditions listed in table I.



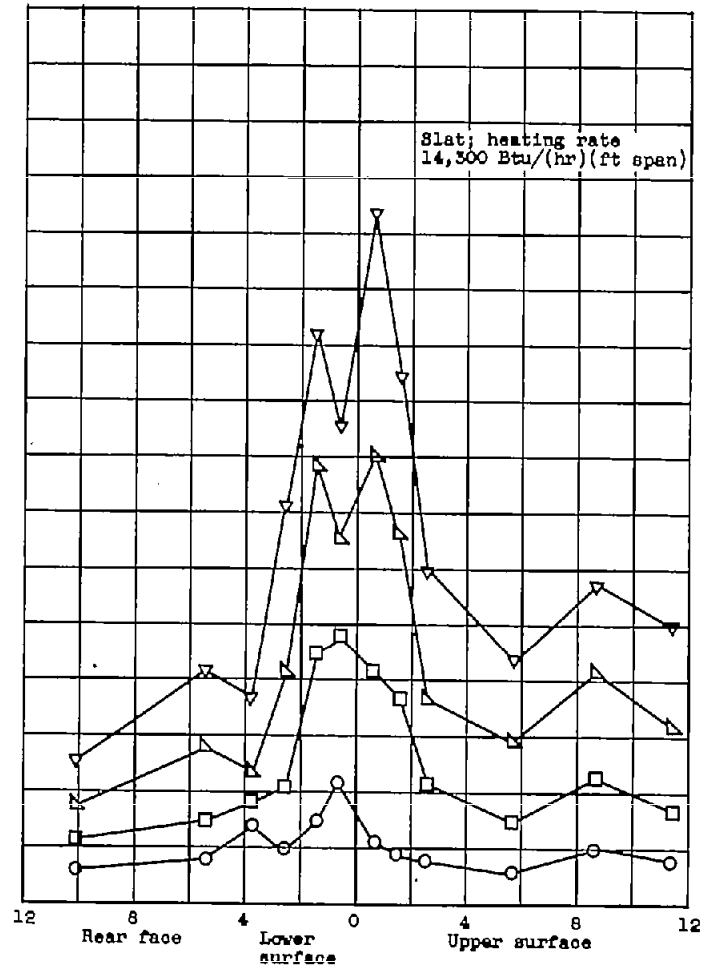
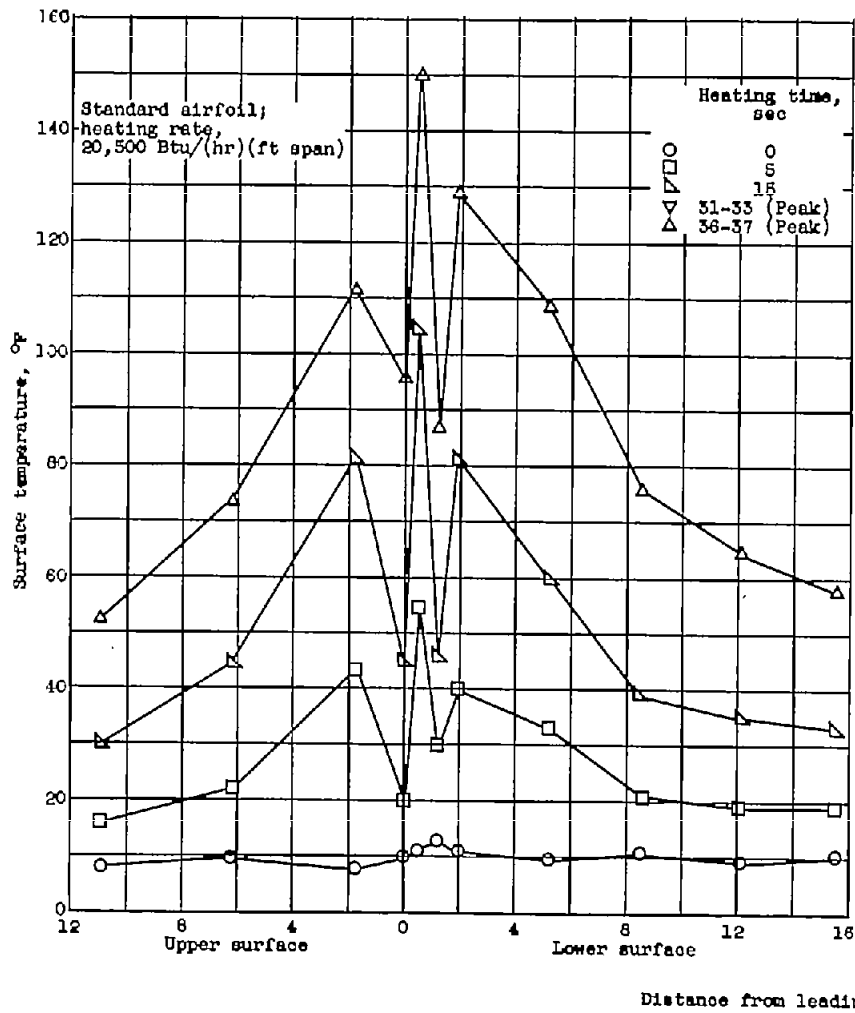
(a) Slat; heating rate, 32,250 Btu/(hr)(ft span); airspeed, 175 mph; datum air temperature, 0° F; angle of attack, 12°; slat open; liquid-water content, 0.55 gram per cubic meter; parting strip heated; gas temperature at valve, 450° F.

Figure 20. - Variation of surface temperature during heating period. Original model; total cycle time, approximately 4 minutes.



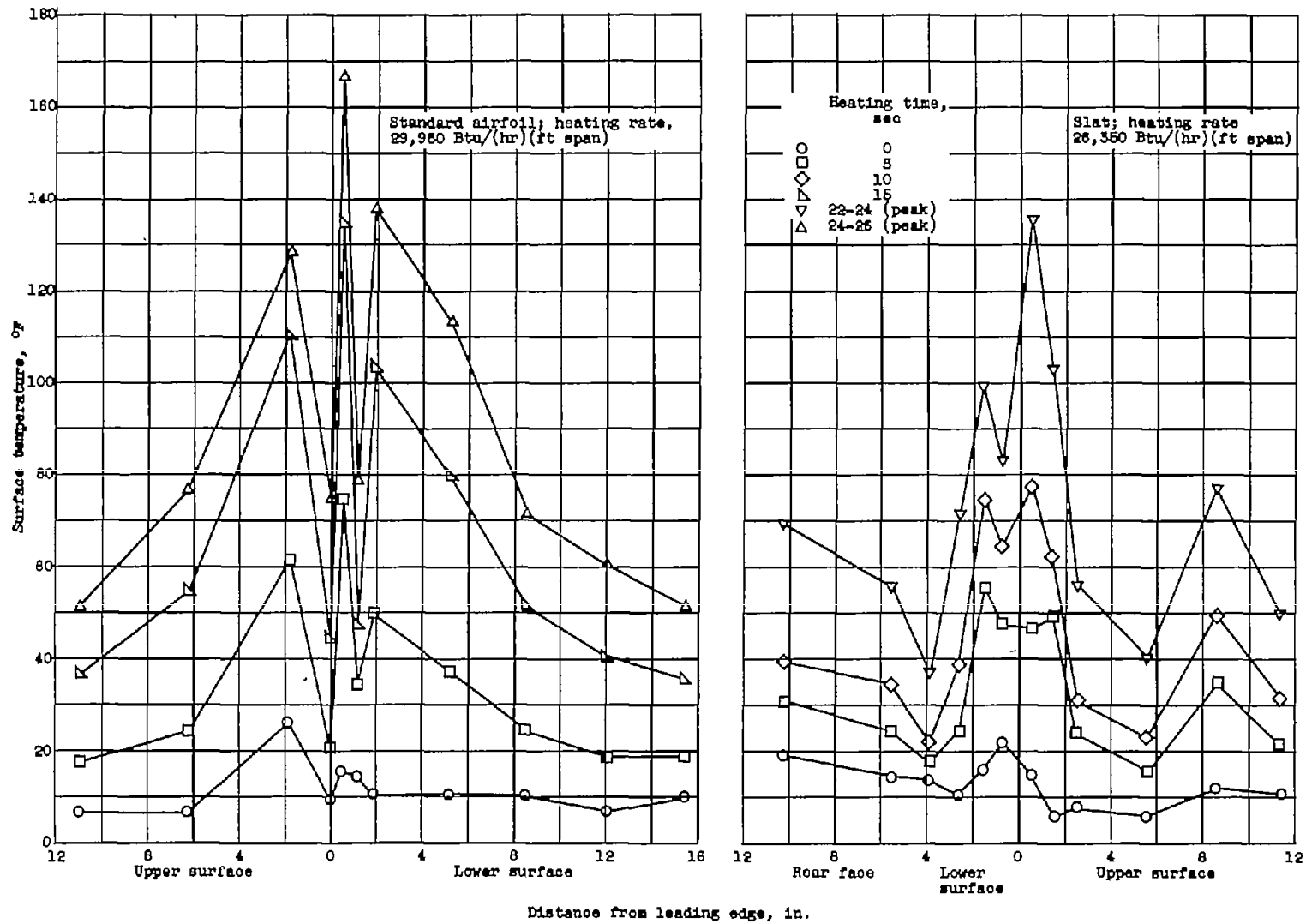
(b) Airspeed, 175 mph; datum air temperature, 10° F; angle of attack, 8°; slat half out; liquid-water content, 0.6 gram per cubic meter; parting strip heated; gas temperature at valve, 450° F.

Figure 20. - Continued. Variation of surface temperature during heating period. Original model; total cycle time, approximately 4 minutes.



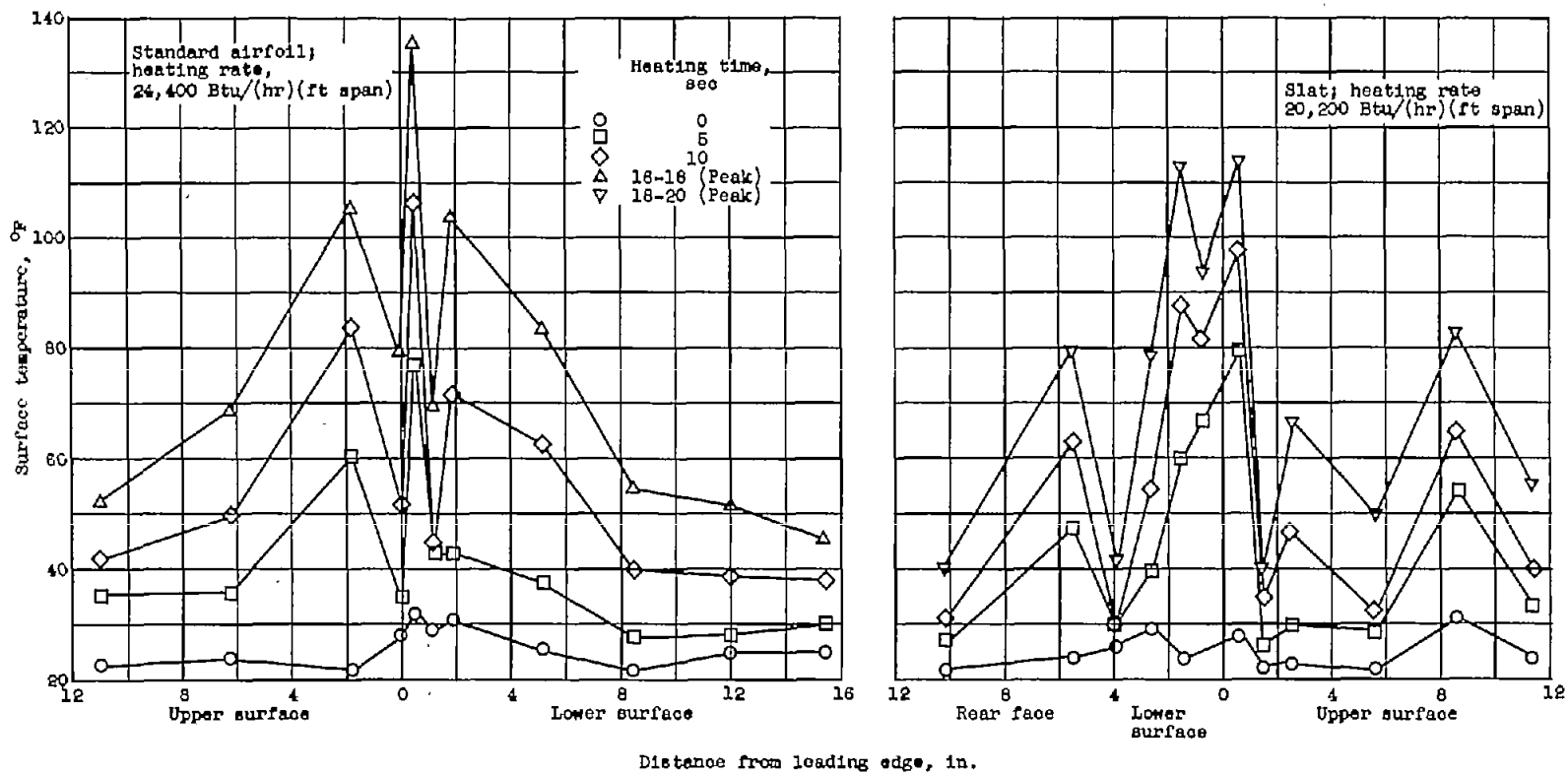
(c) Airspeed, 175 mph; datum air temperature, 10° F; angle of attack, 8°; slat half cut; liquid-water content, 0.6 gram per cubic meter; parting strip unheated; gas temperature at valve, 300° F.

Figure 20. - Continued. Variation of surface temperature during heating period. Original model; total cycle time, approximately 4 minutes.



(d) Airspeed, 250 mph; datum air temperature, 10° F; angle of attack, 4°; slat closed; liquid-water content, 0.5 gram per cubic meter; parting strip unheated; gas temperature at valve, 450° F.

Figure 20. - Continued. Variation of surface temperature during heating period. Original model; total cycle time, approximately 4 minutes.

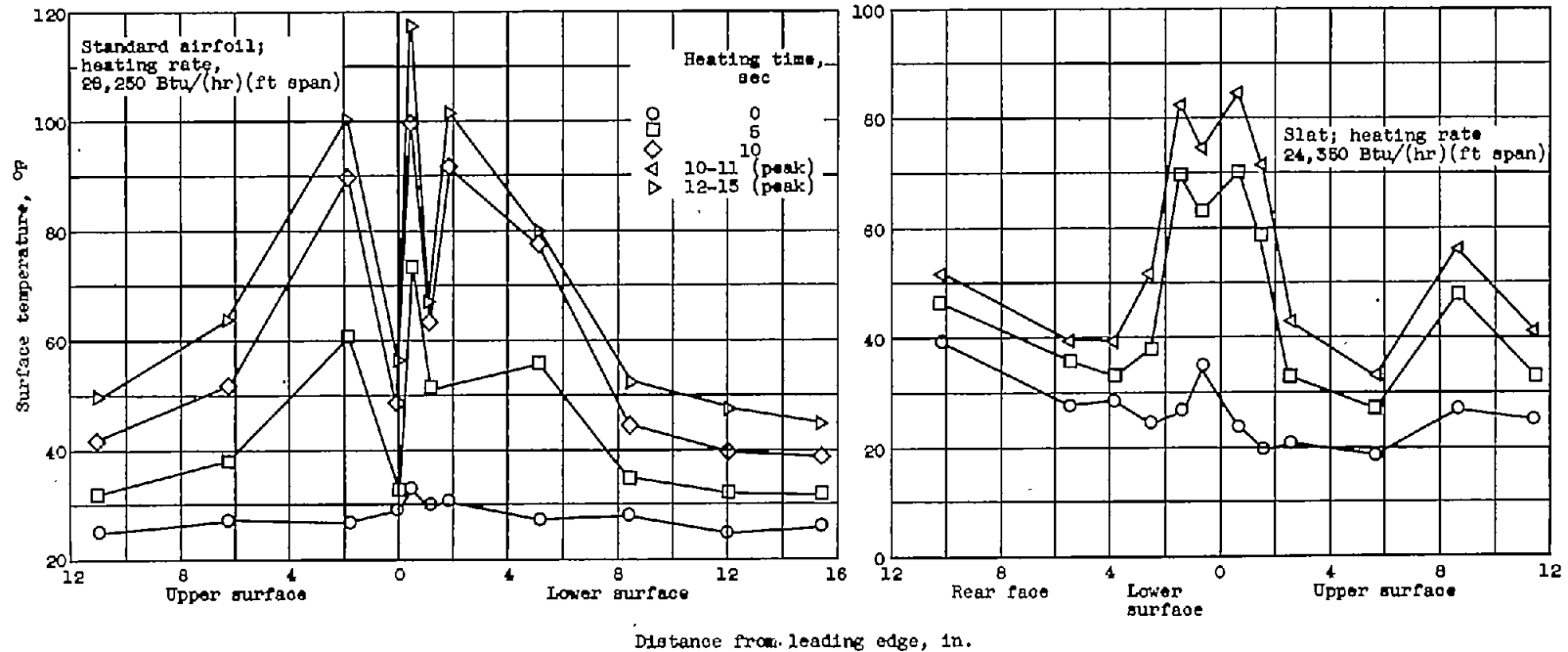


(e) Airspeed, 175 mph; datum air temperature, 25° F; angle of attack, 8°; slat half out; liquid-water content, 1.1 grams per cubic meter; parting strip unheated; gas temperature at valve, 450° F.

Figure 20. - Continued. Variation of surface temperature during heating period. Original model; total cycle time, approximately 4 minutes.

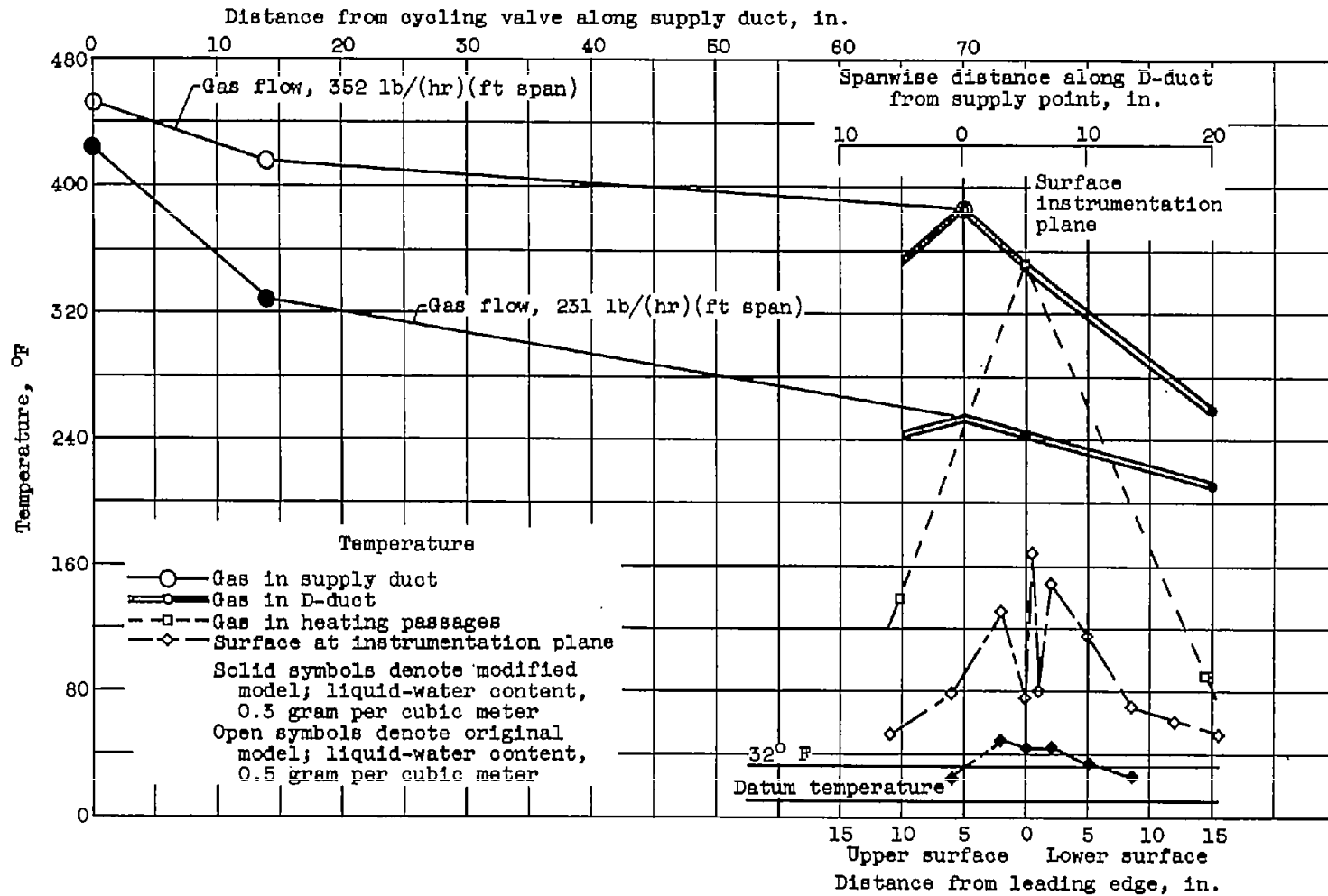
CONFIDENTIAL

CONFIDENTIAL



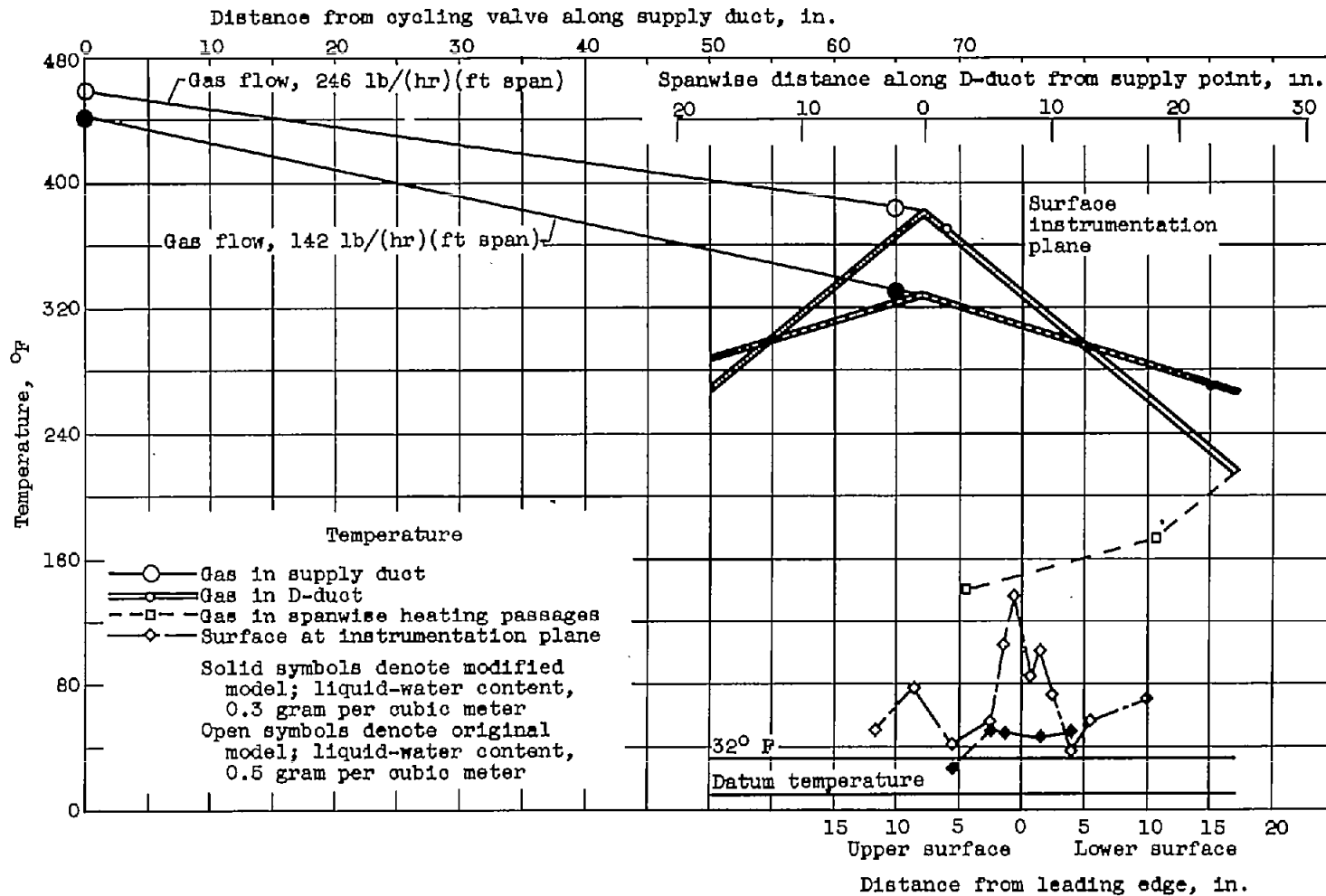
(f) Airspeed, 260 mph; datum air temperature, 25° F; angle of attack, 4°; slat closed; liquid-water content, 0.8 gram per cubic meter; parting strip unheated; gas temperature at valve, 450° F.

Figure 20. - Concluded. Variation of surface temperature during heating period. Original model; total cycle time, approximately 4 minutes.



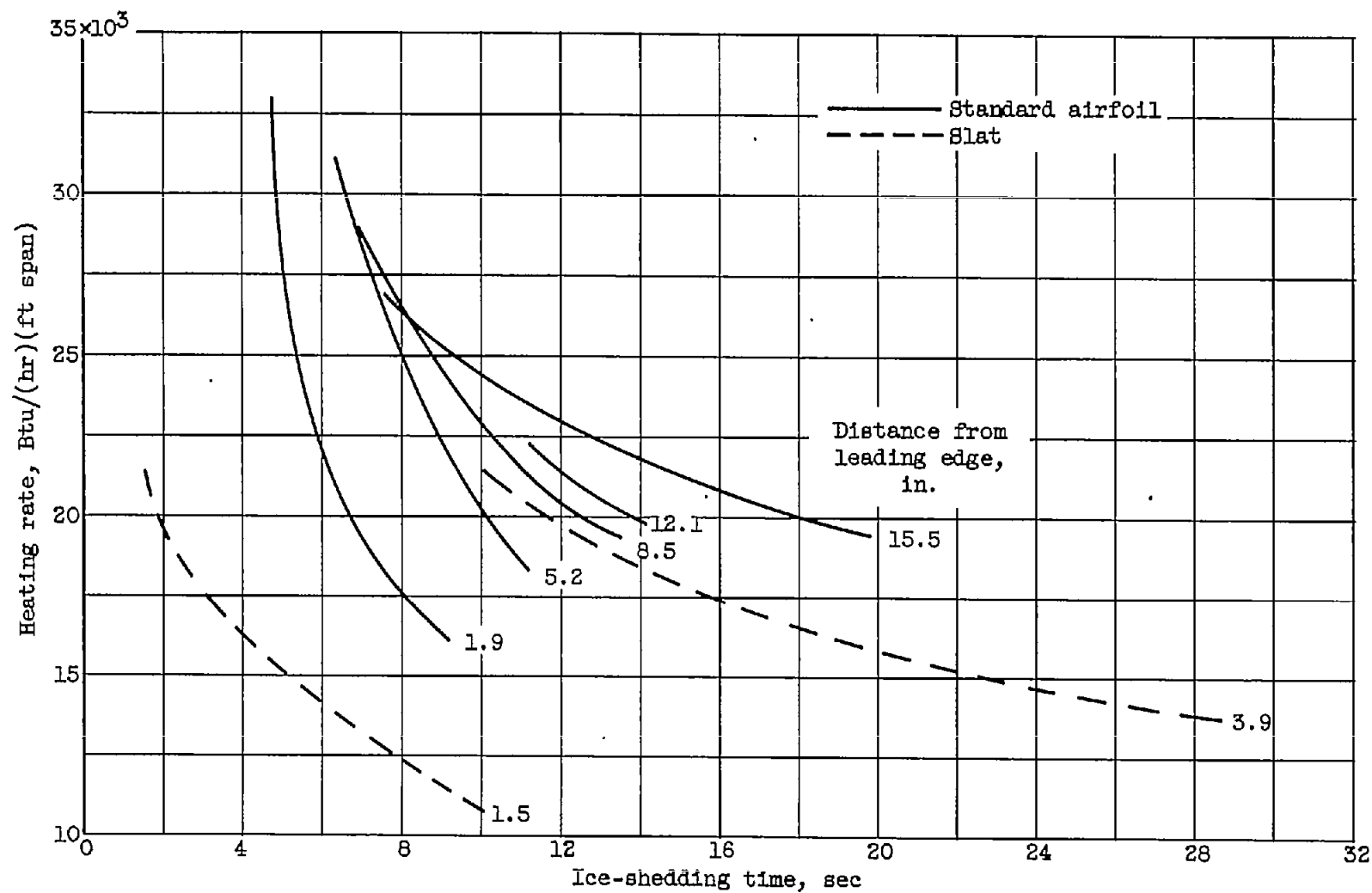
(a) Standard airfoil.

Figure 21. - Variation of gas and surface temperatures with distance for original and modified models at end of heat-on period (peak temperatures) for a typical de-icing condition. Airspeed, 260 mph; datum air temperature, 10° F; angle of attack, 4°; slat closed; heat-on period, 20 to 25 seconds; parting strip unheated.



(b) Slat.

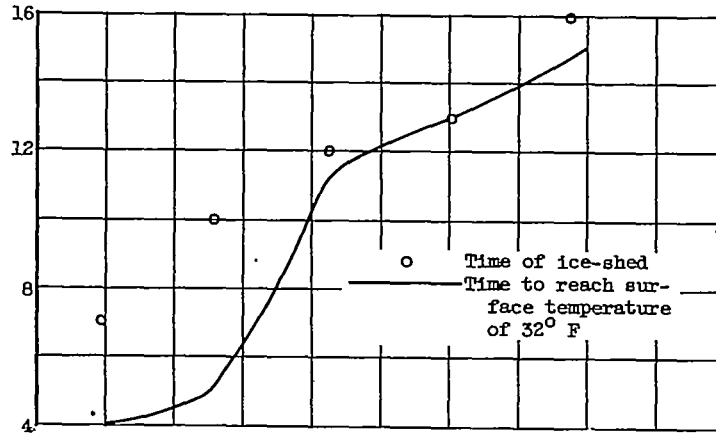
Figure 21. - Concluded. Variation of gas and surface temperatures with distance for original and modified models at end of heat-on period (peak temperatures) for a typical de-icing condition. Airspeed, 260 mph; datum air temperature, 10° F; angle of attack, 4°; slat closed; heat-on period, 20 to 25 seconds; parting strip unheated.



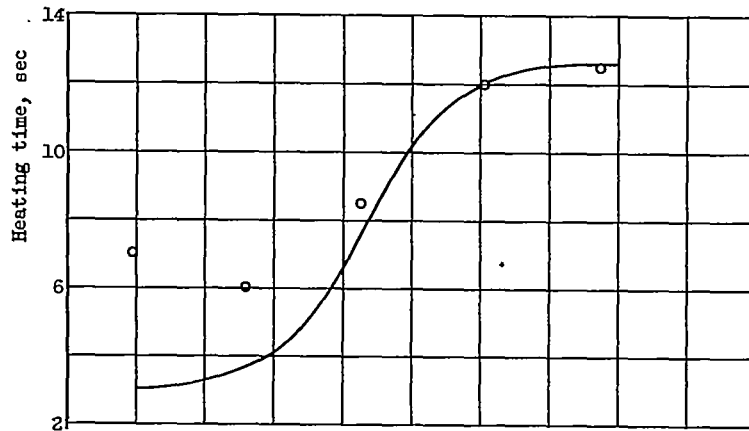
CONFIDENTIAL

Figure 22. - Variation of ice-shedding time with heating rate for several lower-surface locations on original model during marginal de-icing. Airspeed, 175 mph; datum air temperature, 10° F; angle of attack, 8°; slat half out.

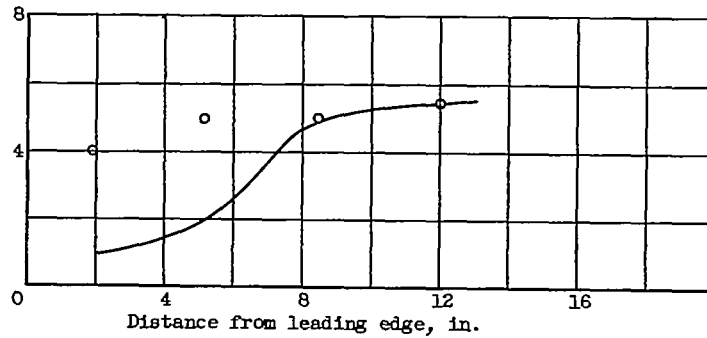
3081



(a) Airspeed, 175 mph; datum air temperature, 10° F; angle of attack, 8°; slat half out; heating rate, 20,500 Btu/(hr)(ft span).



(b) Airspeed, 260 mph; datum air temperature, 10° F; angle of attack, 4°; slat in; heating rate, 29,950 Btu/(hr)(ft span).



(c) Airspeed, 260 mph; datum air temperature, 25° F; angle of attack, 4°; slat in; heating rate, 23,700 Btu/(hr)(ft span).

Figure 23. - Relation of ice-shedding time with time to reach surface temperature of 32° F on lower surface of original standard airfoil.

